Predicting octane number using nuclear magnetic resonance spectroscopy and artificial neural networks

energy&fuels

Combustion

Predicting octane number using nuclear magnetic resonance spectroscopy and artificial neural networks

Abdul Gani Abdul Jameel, Vincent Van Oudenhoven, Abdul-Hamid Emwas, and S. Mani Sarathy

Energy Fuels, **Just Accepted Manuscript** • DOI: 10.1021/acs.energyfuels.8b00556 • Publication Date (Web): 17 Apr 2018

ACS Publications

is published by the American Chemical Society. 1155 Sixteenth Street N.W., Washington, DC 20036

Predicting octane number using nuclear magnetic resonance spectroscopy and artificial neural networks

Abdul Gani Abdul Jameel [*a], Vincent Van Oudenhoven [a,b] Abdul-Hamid Emwas [c], S. Mani Sarathy [a*]

[a] *King Abdullah University of Science and Technology (KAUST), Clean Combustion Research Center (CCRC), Thuwal 23955-6900, Saudi Arabia*

[b] *Department of Computer and Electrical Engineering, University of Waterloo, Waterloo, Ontario, Canada, N2L 3G1*

[c] *King Abdullah University of Science and Technology (KAUST), Imaging and Characterization Core Laboratory, Thuwal 23955-6900, Saudi Arabia*

*Corresponding author:

Abdul Gani Abdul Jameel <abdulgani.abduljameel@kaust.edu.sa>

S. Mani Sarathy <mani.sarathy@kaust.edu.sa>

Abstract:

Machine learning algorithms are attracting significant interest for predicting complex chemical phenomenon. In this work, a model to predict research octane number (RON) and motor octane number (MON) of pure hydrocarbons, hydrocarbon-ethanol blends and gasoline-ethanol blends has been developed using artificial neural networks (ANN) and molecular parameters from ^{1}H nuclear Magnetic Resonance (NMR) spectroscopy. RON and MON of 128 pure hydrocarbons, 123 hydrocarbon-ethanol blends of known composition and 30 FACE (fuels for advanced combustion engines) gasoline-ethanol blends were utilized as a dataset to develop the ANN model. The effect of weight % of seven functional groups including paraffinic CH_3 groups, paraffinic CH_2 groups, paraffinic CH groups, olefinic -$CH=CH_2$ groups, naphthenic CH-CH_2 groups, aromatic C-CH groups and ethanolic OH groups on RON and MON was studied. The effect of branching (i.e., methyl substitution), denoted by a parameter termed as branching index (BI), and molecular weight (MW) were included as inputs along with the seven functional groups to predict RON and MON. The topology of the developed ANN models for RON (9-540-314-1) and MON (9-340-603-1) have two hidden layers and a large number of nodes, and was validated against experimentally measured RON and MON of pure hydrocarbons, hydrocarbon-ethanol and gasoline-ethanol blends; a good correlation (R^2=0.99) between the predicted and the experimental data was obtained. The average error of prediction for both RON and MON was found to be 1.2 which is close to the range of experimental uncertainty. This shows that the functional groups in a molecule or

fuel can be used to predict its ON, and the complex relationship between them can be captured by tools like ANN.

Keywords: RON; MON; functional group; ^{1}H NMR; gasoline ethanol; machine learning

1. INTRODUCTION

Octane number (ON) is a measure of the ignition quality of gasoline and its tendency to resist knocking. Gasolines with high octane numbers are less prone to knocking and can withstand higher compression ratios inside a spark-ignited (SI) internal combustion (IC) engine. Research octane number (RON) and motor octane number (MON) represent the two most commonly employed octane ratings used worldwide. RON is measured by running the fuel in a cooperative fuel research (CFR) engine at standard test conditions as specified by ASTM D2699-16 method [1] and comparing the results obtained with primary reference fuels (PRFs) i.e., mixture of 2,2,4-trimethylpentane (iso-octane) and n-heptane. The compression ratio resulting in knock is measured in the CFR engine and used to evaluate the RON of the test gasoline. MON is also measured in the CFR engine but with a preheated fuel under more intense conditions of engine speed and variable spark timing as specified by ASTM D2700-16a method [2]. Both these standard methods employed for measurement of RON and MON require the use of specialized instrumentation and skilled operators. Also, these methods are time consuming, expensive, and labour intensive. This has led to the development of mathematical models to predict ON, and thus reduce time and costs associated with the experimental measurements.

Several correlations and methods have been reported in the literature to predict ON of pure hydrocarbons [3–6], PRFs [7,8], toluene primary reference fuels (TPRFs) [8–11], gasoline compounds [12], naphtha [13,14], gasolines [15–22], gasoline with ethanol [7,23–27] and petroleum fractions [16]. The inputs for these models have been generated by utilizing different analytical techniques such as Fourier transform infra-red (FT-IR) spectroscopy [5,13,28,29], flame emission spectroscopy [30], nuclear magnetic resonance (NMR) spectroscopy [23,31,32], dispersive fiber-optic Raman spectroscopy [19], dielectric spectroscopy [18], gas chromatography [17], distillation curves [15], thermal wave interferometry [21] and ignition delay time (IDT) measured in an ignition quality tester (IQT) [22]. The data from these

techniques have been analysed by a number of statistical and theoretical methods like multiple linear regression (MLR) [23], partial least square (PLS) [30], quantitative structure property relationship (QSPR) [3,4], response surface methodology [10,33] and artificial neural networks (ANN) [6,33–35] to process the data and yield the prediction models.

The required gasoline RON and MON for a specific vehicle depends on the engine type and operating conditions [36]. Since RON and MON measurements are made on standard CFR engines under pre-defined standard conditions, the fuel metrics are a direct result of the fuel's physical and chemical properties. In the present work, a model has been developed to predict the RON and MON of gasolines containing oxygenates (ethanol) by utilizing the fuels chemical composition expressed in terms of functional groups. Real fuels like gasolines contain several hundred individual molecules and identifying and quantifying all of them is difficult. However, these fuels are made up of a finite number of functional groups which are responsible for their properties (i.e. derived cetane number (DCN) [37,38], sooting propensity [39] [40], flame speed [41,42], flash point [43] etc.) Determining these functional groups using analytical methods like ^{1}H NMR spectroscopy presents a convenient way of characterizing the chemical composition of these fuels and also in predicting their properties. Gasolines are usually composed of the following hydrocarbon classes: paraffins, *iso*-paraffins, olefins, naphthenes and aromatics. Seven functional groups derived from the above hydrocarbon classes, namely weight % of paraffinic CH_3 groups, paraffinic CH_2 groups, paraffinic CH groups, olefinic CH-CH_2 groups, naphthenic CH-CH_2 groups, aromatic C-CH groups and ethanolic OH groups, were used an input to the model along with molecular weight and a new parameter called as branching index (BI), a quantity that describes the degree of branching in a molecule while considering the position of the methyl branch.

The BI is defined as 0 for n-paraffinic molecules. The BI for iso-paraffins, is defined as per Equation (1).

$$BI_{i-p} = \frac{Number\ of\ C\ atoms\ connected\ to\ the\ longest\ chain + PI\ of\ each\ C\ connected\ to\ the\ longest\ chain}{Number\ of\ C\ atoms\ in\ the\ longest\ chain} \quad (1)$$

Where PI is called as the position index. The position of the methyl branch in a molecule correlates with its properties. For example, RON/MON (73.4/73.5) of 2-methylpentane is lesser compared to RON/MON (74.5/74.3) of 3-methylpentane. Similarly DCN of 2-methylpentane

(34.5) is different compared to the DCN of 3-methylpentane (30.7). Both these molecules are isomers and have similar functional group distribution. These differences are true for all iso-paraffinic molecules. PI is defined as per Equations (2) – (4).

$$PI = 0, if\ the\ C\ atom\ is\ connected\ to\ the\ outermost\ position\ of\ the\ longest\ chain \quad (2)$$

$$PI = 0.5, if\ the\ C\ atom\ is\ connected\ 1\ position\ away\ from\ the\ outermost\ position\ of\ the\ longest\ chain \quad (3)$$

$$PI = 0.5 + 0.5\ , if\ the\ C\ atom\ is\ connected\ 2\ positions\ away\ from\ the\ outermost\ position\ of\ the\ longest\ chain\ and\ so\ on \quad (4)$$

For example, let us calculate the BI of 3-methylpentane which has 5 C atoms in its longest chain. This is connected to 1 C atom (3-methyl) one position away from the outermost position on the longest chain. As a result it has a PI of 0.5 and BI of 3-methylpentane is computed as 0.3. The present definition of BI helps to explain the different properties of 2-methylpentane which has a BI of 0.2. The BI of olefins is computed similar to *iso*-paraffins. For, ringed structures like napthenes and aromatics with alkyl side chains, the BI is calculated by redrawing the molecular structure to iso-paraffins. For more detailed information on how to calculate the BI please refer to [37].

The chemical kinetic reactivity of the fuel, which is dependent on molecular structure, governs ignition of gaseous air/fuel mixtures. The nine parameters used in the present work contain the necessary molecular information to explain chemical properties affecting gas-phase kinetic reactivity. Therefore, characterizing the fuel qualitatively and quantitatively in terms of the chemical functionalities present in the fuel can help predict both RON and MON. The present functional group approach of predicting fuel properties has been successfully applied to predict the DCN of hydrocarbon fuels by Abdul Jameel et al [37]. The above mentioned functional groups have also been used to formulate surrogates for gasolines, diesel and jet fuels in a method called as the minimalist functional groups (MFG) approach [44,45]. ^{1}H NMR spectroscopy was utilized to identify and quantify the different functional groups present in the

fuel. The various functional groups have distinct peaks in the NMR spectra and they can be quantified by integrating the peaks.

Artificial neural networks (ANN) are statistical machine learning tools that have the ability to 'learn' complex relationships between inputs and outputs in a given dataset. The predictive capability of methods like PLS and MLR was found to be limited when applied to RON and MON, especially in gasolines containing ethanol [23]. There is a non-linear increase in RON and MON of a gasoline when ethanol (an octane booster) is blended [26]. Therefore, ANN was employed to effectively capture non-linear and complex relationships between input features and the output of interest (RON and MON). ANN are computational models consisting of interconnected nodes that represent "features" or attributes of the analyzed dataset, which form a network that, if "trained" appropriately, can encompass the relationship between inputs and outputs of interest. These nodes are structured in layers depicted in figure 1. Each ANN has a single 'input layer', one or more 'hidden layers', and a single 'output layer'. The number of units in each layer can be varied. Apart from the nodes in the input layer, which are the original features supplied, a node in a particular layer is comprised of each node in the layer right before it. For example, a node in the 'hidden layer' is comprised of the nodes in the input layer (represented by the arrows in figure 1). As more hidden layers are added to the network, the subsequent nodes become more and more complex combinations of the original inputs (and what they represent becomes exponentially more convoluted). Each node has an associated weight that is directly proportional to the influence of that particular feature on the final output of the network.

In this work, ANN models are used to analyze the relationship between the above nine parameters for predicting RON and MON of pure hydrocarbons, hydrocarbon-ethanol and gasoline-ethanol blends. The ANN model was developed using a dataset comprising experimental ONs of pure hydrocarbons, blends of hydrocarbons and gasolines with ethanol. ^{1}H NMR spectroscopy was employed to obtain the functional groups of gasoline-ethanol fuel mixtures. The developed ANN models were then validated against a separate test set of experimental data.

2. FUNCTIONAL GROUP DETERMINATION

For pure hydrocarbons and hydrocarbon-ethanol blends, the nine input parameters (seven functional groups, BI and MW) can be calculated directly from the molecular structure and the compositional data. For example, n-heptane (MW= 100 g/mol) is composed of 2 paraffinic CH_3 groups (MW= 15 g/mol) and 5 paraffinic CH_2 groups (MW= 14 g/mol). The weight % of paraffinic CH_3 groups and paraffinic CH_2 groups in n-heptane is 30 and 70, respectively. For a PRF mixture (n-heptane 40 vol%, 2,2,4-trimethylpentane 60 vol%), TPRF mixture (n-heptane 40 vol%, 2,2,4-trimethylpentane 45 vol%, toluene 15 vol%) and TPRF + ethanol mixture (n-heptane 40 vol%, 2,2,4-trimethylpentane 35 vol%, toluene 15 vol%, ethanol 10 vol%) the functional groups (in weight %) can be calculated with the knowledge of density of the individual species. The calculated functional groups for the above 3 mixtures are presented in figure 2.

For real fuels like gasolines or gasolines containing ethanol, the functional groups can be calculated from their ^{1}H NMR spectra. The ^{1}H NMR experiments of six FACE gasoline fuels (FACE A, C, F, G, I, J) and their ethanol blends were performed using Bruker 700 AVANAC III spectrometer equipped with Bruker CP TCI multinuclear *CryoProbe* (BrukerBioSpin) at 298 K. Samples were prepared by dissolving 50 µl of the fuel in 700 µl of deuterated chloroform $CDCl_3$. The spectra were recorded using a recycle delay time of 5s. The standard 1D 90^o pulse sequence using the standard (zg) program from Bruker pulse library was used and 128 scans were collected. Chemical shifts were adjusted using Tetramethylsilane (TMS) as an internal chemical shift reference and the spectra were processed using Bruker Topspin 2.1 software. The ^{1}H NMR spectra are represented in terms of chemical shifts, usually between 0 – 12 ppm. Each functional group gives rise to a distinct peak in the spectra at their characteristic chemical shift region and integrating the individual peaks enables their quantification relative to other groups. The characteristic ^{1}H NMR structural assignments of the functional groups are presented in Table 1. The quantity of a particular type of proton (H atom) in the sample (in mole %) can be calculated from the integral intensity of the corresponding peak divided by the integral intensities of all the peaks in the spectra, and then multiplying by 100. The quantity of the functional groups (in weight %) can then be deduced by the number of C and H atoms and

molecular weight of the group. For example, paraffinic CH_2 groups possess two H atoms for each C atom. Their quantity in the sample (in weight %) can then be calculated by the product of mole % of the H atoms that give rise to paraffinic CH_2 peaks (namely D and H, see Table 1) with the molecular weight (i.e., 14) and dividing the total by the number of H atoms in the paraffinic CH_2 group (i.e., 2). The formulae required to calculate the functional groups discussed above are reported in Table 2.

Other inputs for the model, besides the functional groups, namely the branching index (BI) of the gasoline fuels can also be calculated from their ^{1}H NMR spectra using the Equation (5) given below.

$$BI_{gasoline} = \frac{I/3+J/3+K/2}{H/2+G} + \frac{A}{T*4} + 0.5 * \frac{F}{T*10} + \frac{E/3+(L+M)/3}{D/2+C} \quad (5)$$

The explanation of the terms in the above equation is provided in Table 1. More detailed information regarding the definition and derivation of the above Equation can be obtained from Abdul Jameel et al [37]. The MW of gasolines (which usually lies between 90-130 g/mol) can be calculated from theoretical methods [46] using the ASTM distillation curve data and specific gravity or from experimental methods like vapor pressure osmometry [47,48].

3. ANN TRAINING METHODOLOGY

The RON and MON of 128 pure hydrocarbons comprising of n-paraffins, iso-paraffins, olefins, naphthenes and aromatics (see Table 3), 123 hydrocarbons blended with ethanol (see Table 4) and 30 FACE (fuels for advanced combustion engines) gasolines blended with ethanol (see Table 5) were collected from literature. The nine input parameters (seven functional groups, molecular weight, and branching index) were calculated for each of these 281 entries and were used as the dataset to predict RON and MON. ANN models were chosen to capture the non-linearity and the presumed complexity between the input features and RON and MON, whilst keeping prediction as priority.

The data was split into a randomly generated validation set containing 57 points and a training set containing 225 points, in a 20/80 split. The fixed test set was used for the final evaluation of the RON and MON ANN models. The ANN models were designed using the tools

made available by Keras, a deep-learning library on top of Theano, and optimization of the models was performed using an in-house python code. In order to "tune" the ANN model, a continuous evaluation method is required. Adjusting the model directly on the test set leads to information from the test set leaking in to the final model, resulting in misrepresentative error metrics. This is why a separate set, the "validation set" was used exclusively for evaluating the model during fine-tuning. Due to the size of the dataset and its broad domain, defining a separate validation set would have led to a significant drop in overall learning capabilities. Instead K-fold Cross Validation (CV) was used. Not only is this a reliable validation method, it can also overcome the innate variance of the dataset to some degree, as the amount of information extracted from the dataset is maximized without prioritizing certain examples over others.

Firstly, the training set was split up in to K number of "folds" or subsamples, one of which was chosen as the validation fold, while the others were used for the training of the model. This was rotated until each fold had been tested on. The evaluation of the model consists of the average over the K tested folds. Based on this evaluation, the following hyper parameters were tuned: the number of units per layer, regularization (common method for combating overfitting) coefficients, and the number of layers. Each node in the network has an associated weight that is directly proportional to the influence of that particular feature. For this study, feed forward neural networks [49] were used, wherein the data moves in a single direction: from the input layer to the output. After a certain number of iterations, also known as epochs, of the above process, a local minima was found for the specific ANN and dataset. Multiple feed forward architectures (topology of the model) were tested to arrive at the models that gave the best results. Finally, the ANN was retrained on all the folds (the original training set) and evaluated on the test set, which lead to a robust model. More information on the ANN methodology adopted is provided as Supporting Information.

4. RESULTS & DISCUSSION

Gasoline octane rating depends on the fuel's chemical composition [50]. n-Paraffins have shorter ignition delays compared to aromatic and naphthenic molecules of the same C

number due to the rapid radical chain branching initiated by low-temperature oxidation reactions. Aromatic molecules are more knock resistant and display longer ignition delays due to their stabilized radical intermediates. The effect of the functional groups that make up these molecules on RON and MON is discussed below.

4.1 Paraffinic CH_3 groups

The occurrence and the degree of methyl substitution has a great impact on the ignition of paraffinic fuels as experimentally shown by Lapuerta et al. [51]. Experiments performed on mixtures of C_{16} isomers (n-hexadecane, 2,6,10-trimethyltridecane and heptamethylnonane) in a constant volume combustion chamber showed that increasing methyl branches resulted in an increase in ignition delay [51]. Low temperature chain branching reactions are also inhibited by methyl substitution [52]. Figure 3 shows the effect of paraffinic CH_3 groups in hydrocarbon-ethanol and gasoline-ethanol blends on their RON and MON. It can be seen that as the paraffinic CH_3 content increases, both RON and MON generally continue to decrease. In blends of 1,2,4-trimethylbenzene and ethanol we see an opposing trend. When ethanol is added to 1,2,4-trimethylbenzene, RON of the mixture reduces due to antagonistic effects, and its value is lower than the individual ON of both the molecules. The CH_3 content of 1,2,4-trimethylbenzene (37.5 wt %) is slightly higher than that of ethanol (32 wt %), and addition of ethanol reduces the overall CH_3 content while simultaneously reducing both RON and MON. Addition of ethanol to TPRF 3 blends does not change the CH_3 content significantly, so RON and MON increase due to ethanol's octane boosting effect. For FACE J gasoline blended with ethanol, we see an increase in RON/MON with increase in CH_3 content. This is because FACE J gasoline contains lower CH_3 content (25.4 wt %) than ethanol and also lower than the other FACE gasolines analyzed in the study.

4.2 Paraffinic CH_2 groups

Paraffinic CH_2 and CH_3 groups play a major role in the combustion characteristics of paraffinic fuels [53]. Generally the lengthening of the main chain in n-paraffins or iso-paraffins (increasing CH_2 content) leads to decrease in the ignition delay time and therefore tends to decrease the octane number of the molecule. The mass ratio of CH_2/CH_3 groups has been

experimentally shown to be a governing parameter in auto-ignition reaction of paraffins by performing experiments with C_{16} isomers with the same CH_2/CH_3 ratio [51]. CH_2 groups have been identified along with CH_3 and benzyl groups as constraints that effect the gas phase combustion of jet fuels [54]. The effect of paraffinic CH_2 groups on RON/MON of pure hydrocarbon-ethanol and gasoline-ethanol blends is shown in figure 4. As the paraffinic CH_2 content increases, RON/MON decreases in all the pure hydrocarbon blends. There is an increase in RON/MON in FACE A, F and G gasoline-ethanol blends. This is because ethanol addition brings about a net decrease in the paraffinic CH_2 content of the mixture.

4.3 Paraffinic CH groups

Octane rating generally increases by the addition of a side chain in a paraffin or an olefinic molecule. The position of the alkyl side chain also affects the ON of the molecule. Particularly, introduction of a branch (CH group) in the center of a paraffin or olefin results in the increase of RON/MON. Paraffinic CH groups have lower bond dissociation energy compared to paraffinic CH_2 and CH_3 groups which reduces the energy barrier for H-atom abstraction and migration reactions. In addition, introducing methyl substitutions hinders low temperature reactions leading to ignition [55–59]. Figure 5 shows the effect of paraffinic CH groups on RON/MON of hydrocarbon-ethanol and gasoline-ethanol blends. It can be observed throughout that RON/MON decreases with increase in paraffinic CH groups. This unexpected trend is because ethanol does not contain any paraffinic CH group, and its addition to both the hydrocarbon blends and gasolines reduces paraffinic CH content of the mixture. Because the hydroxyl functionality is so effective at inhibiting reactivity, decreasing paraffinic CH content by ethanol addition serves to increase the RON/MON.

4.4 Olefinic $-CH=CH_2$ groups

The ON of olefins are usually greater than their corresponding paraffins/iso-paraffins of the same carbon number because olefinic functional groups are comparatively less reactive. Olefins are sometimes present in gasoline fuels in small fractions and have a major effect on the autoignition characteristics and their oxidative stability. At high temperatures (> 1000 K)

oxidation commences by abstraction of allylic H atoms which are in a β position to the double bond. The position of these double bonds also affects their ON. The effect of olefinic –CH=CH_2 groups present in hydrocarbon-ethanol and gasoline-ethanol blends on their RON/MON is shown in figure 6. It can be observed throughout the blends that as the olefinic groups increase, RON/MON continue to decrease, which again indicates that ethanol addition decreases olefinic content but increases antiknock quality.

4.5 Naphthenic –CH-CH_2 groups

Gasolines usually contain naphthenes (< 20 vol %) and their molecular formula is similar to mono-alkenes but their combustion chemistry is significantly different due to their ringed structures. Naphthenes generally have higher ON compared to n-paraffins, iso-paraffins and olefins of the same carbon number (e.g., comparing cyclopentane and other C5 hydrocarbons [60,61]. The ON of naphthenes can be increased by converting them into aromatics via dehydrogenation, and naphthenes possess high sooting tendency due to their propensity to form aromatic rings. The combustion of chemistry of naphthenes is similar to that of n-paraffins. At high temperatures, cycloalkyl radicals are formed and subsequent ring-opening results in the formation of dienes. At low temperatures, the cycloalkyl radicals form alkylperoxy radicals after reacting with O_2. Figure 7 shows the effect of variation of naphthenic –CH-CH2 groups on RON/MON of hydrocarbon-ethanol and gasoline-ethanol blends. When the naphthenic groups reduce due to the addition of ethanol, the RON/MON of the fuel increases in all the mixtures studied.

4.6 Aromatic C-CH groups

Aromatic groups increase the octane rating of the fuel by increasing the ignition delay time. Aromatic molecules have higher RON/MON (and sensitivity) compared to their corresponding napthenic molecules with the same carbon number. Toluene has a higher RON/MON (118/100.3) compared to methylcyclohexane (89.2/72), respectively. The addition of alkyl chains to an aromatic tends to reduce the ON of the molecule. The low and intermediate temperature combustion chemistry of aromatics is significantly different than that of paraffins/ iso-paraffins. H atoms bonded to aromatic rings have high bond dissociation

energies that hinder initiation reactions. However, H atoms in alkyl chains connected to the aromatic rings are easier to abstract. The effect of aromatic C-CH groups on the RON/MON of hydrocarbon-ethanol and gasoline-ethanol blends is shown in figure 8. The addition of ethanol results in a net reduction of the aromatic C-CH groups, which should lead the observer to expect a reduction in both RON and MON, but however a steady increase in RON and MON is seen. This is because, while the aromatic C-CH groups decrease, the ethanol OH group increases steadily and compensates for the octane boosting nature of the aromatic groups. This shows that ethanol's OH group has a more dominant effect on octane boosting compared to all other functional groups studied here.

4.7 Ethanol OH group

As shown by the results above, a unit increase of ethanol OH groups in the fuel has a greater effect on RON/MON compared to the other groups. This is because ethanol reacts with OH radicals to primarily form CH_3CHOH radicals. The OH group connected to the hydrocarbon chain in ethanol weakens the bond strength of the adjacent CH_2 making it easy to abstract [62]. The alpha-hydroxyethyl radicals undergo a chain termination pathway; they react with O_2 to form acetaldehyde and HO_2 radical. Therefore, ethanol addition acts as a radical scavenger and leads to the reduction of low temperature heat release (LTHR) and the reactivity of the fuel [63]. Figure 9 shows the effect of ethanol OH groups on the RON/MON of hydrocarbon-ethanol and gasoline-ethanol blends. It can be observed that as the ethanol OH groups increase, RON/MON increase except for the 1,2,4-trimethylbenzene-ethanol blends as discussed in section 3.1.

4.8 Molecular weight

The ON of a molecule generally decreases with increase in its molecular weight. This is valid for all cases of n-parafffins. For iso-paraffins, ON generally decreases with increasing size provided the degree of branching remains the same. Gasolines typically have a molecular weight in the range (≈ 100 g/mol) with average carbon number of 7. Aromatics comprise the highest molecular weight compounds present in gasolines in C_6 – C_9 range. Average molecular weight of gasoline has a major effect on its physical properties. The effect of molecular weight

on the RON/MON of hydrocarbon-ethanol and gasoline-ethanol blends is shown in figure 10. It is observed that when the molecular weight of the mixtures increases, RON/MON decreases.

4.9 Branching Index (BI)

Branched paraffins of the same carbon number show an increase in the ON when the degree of branching increases. Also the position of the branch (or methyl substitution) has an effect on the reactivity of the molecule. RON/MON of 2,2-dimethylbutane and 2,3-dimethylbutane is 91.8/93.4 and 100.3/94.3, respectively. These molecules have the same distribution of functional groups, molecular weight and CH_3/CH_2 ratio. The BI term defined in our previous work [37] quantifies the 'degree' of branching and also incorporates a position index (PI) to account for the effect of the position of the methyl substitution. Also, an expression was developed to calculate the branching index of gasolines from their ^{1}H NMR spectra. Figure 11 shows the effect of branching index on the RON/MON of hydrocarbon-ethanol and gasoline-ethanol blends. As per the definition, ethanol has a BI of 0 and its addition reduces the overall BI of the mixture.

4.10 ANN Model

The test data comprised of 57 points (20 % of the data) that were randomly selected to validate the developed ANN model comprising of pure hydrocarbons, hydrocarbon-ethanol blends and FACE gasoline –ethanol blends. A distinct model was constructed for both RON and MON using the same initially defined training and test sets. The topology of the final models are expressed as units in each layer separated by a dash; the first unit represents the input layer, the last unit refers to the output layer, and the middle two units represent the hidden layers. The topology and error metrics are presented in Table 6. There is good comparison between the experimental and the predicted values of RON and MON as shown in figure 12. The value of the regression coefficient (R^2) obtained for both the cases was 0.99. Some of the points showed an absolute error of prediction of up to 6. The most likely reason for these outliers is that they could be statistically unique when compared to the rest of the dataset. When training the ANN, the relationships found between the input features and the output of interest are going to be those that are most prominent. If there are a few data points that do not fit this trend, or which

have particular properties that are relatively unique, then the ANN may struggle in predicting their values accurately. The mean absolute error of prediction for RON and MON for the test set was found to be 1.2 for both, which is near the vicinity of experimental error (0.7) while measuring per the ASTM standard CFR methodology.

The majority of predictive models [23,34,64,65] in the literature use MLR for simplicity and ease in developing the model from a given dataset. MLR develops a mathematical relation between a dependent variable (ON) and a number of independent variables (the nine functional group parameters used herein) in the form of a straight line equation that best fits all the points in the dataset. A separate model for RON and MON, was also developed using MLR with the present dataset and presented in Equations (2) and (3), respectively.

$$RON = 44.82 + 0.86 * paraffinic\ CH_3\ (wt\ \%) + 0.25 * paraffinic\ CH_2(wt\ \%) + 0.23 * paraffinic\ CH(wt\ \%) + 0.76 * olefinic - CH = CH_2(wt\ \%) + 0.43 * naphthenic\ CH - CH_2(wt\ \%) + 0.56 * aromatic\ C - CH(wt\ \%) + 1.22 * ethanolic\ OH(wt\ \%) - 0.31 * MW + 26.69 * BI \quad (2)$$

$$MON = 31.26 + 0.86 * paraffinic\ CH_3\ (wt\ \%) + 0.29 * paraffinic\ CH_2(wt\ \%) + 0.26 * paraffinic\ CH(wt\ \%) + 0.49 * olefinic - CH = CH_2(wt\ \%) + 0.40 * naphthenic\ CH - CH_2(wt\ \%) + 0.49 * aromatic\ C - CH(wt\ \%) + 0.94 * ethanolic\ OH(wt\ \%) - 0.22 * MW + 28.47 * BI \quad (3)$$

As seen from figure 13, there is a poor comparison between the measured and MLR predicted values, wherein R^2 for RON and MON are 0.52 and 0.51, respectively. This is mostly due to the antagonistic effect of ethanol addition[23,24,26,63,66], which a linear MLR model is unable to capture.

Octane sensitivity (OS)[67], defined as the difference between RON and MON, is a measure of the difference in auto-ignition chemistry between that of the fuel and PRF. High octane sensitive fuels are more resistant to knock and are of interest in modern SI engines. The measured and predicted sensitivity of fuels are shown in figure 14. As seen, the ANN models are also able to capture the octane sensitivity of the fuels in the dataset. The mean absolute

error of prediction of the octane sensitivity is 1.4, which is also close to the level of experimental error.

This shows that the ON of pure hydrocarbons, blends, oxygenated gasoline fuels etc. can be predicted by knowledge of the functional groups comprising them. Also, ANN can be as used a successful tool to establish a relationship between ON and functional groups along with BI and molecular weight. The developed ANN model can be used to predict the octane numbers of pure hydrocarbons and blends. It can also be used to design fuels of specified RON and MON targets. The ON of oxygenated gasoline fuels can be predicted with knowledge of the ^{1}H NMR spectra. These models are implemented in the Fuel Design Tool on CloudFlame [68,69] (cloudflame.kauste.edu.sa) cyber-infrastructure developed by KAUST and Saudi Aramco for predicting RON and MON. A list of standard molecules are also included in the tool; entering the composition in vol % or mol % of a known blend calculates he input parameters as well as RON and MON values of the blend. For real fuels like gasolines, the RON and MON can be automatically computed by uploading the ^{1}H NMR spectra of the fuel.

5. CONCLUSION

An ANN based model was developed to predict the RON and MON of pure hydrocarbons, hydrocarbon-ethanol blends and gasoline-ethanol blends. Seven functional groups namely paraffinic CH_3 groups, paraffinic CH_2 groups, paraffinic CH groups, olefinic -$CH{=}CH_2$ groups, naphthenic CH-CH_2 groups, aromatic C-CH groups and ethanol OH groups along with branching index (BI) and molecular weight were utilized as inputs of the model. A dataset comprising of 281 points (128 pure hydrocarbons, 123 hydrocarbon-ethanol blends and 30 gasoline-ethanol blends) was used and the nine inputs for each of these points was calculated. The developed ANN models with two hidden layers and a high number of nodes for both RON (9-540-314-1) and MON (9-340-603-1) resulted in the lowest error metrics. The model was validated against a separate test set comprising 20% of the original data set and there was a good accuracy of prediction for both RON and MON (R^2=0.98). The mean absolute error of prediction for RON and MON was found to be 1.2 which is close to the experimental measurement error. The developed ANN models can be used to predict the ON of pure hydrocarbons, hydrocarbon-

ethanol and gasoline- ethanol blends by knowledge of the functional groups, branching index (BI) and molecular weight.

Acknowledgement

This work was supported by the Saudi Aramco R&DC and Clean Combustion Research Center (CCRC) at King Abdullah University of Science and Technology (KAUST) under the FUELCOM Research Program. The work was also funded by KAUST competitive research funding awarded to the CCRC.

References

[1] ASTM Int. Standard Test Method for Research Octane Number of Spark-Ignition Engine Fuel 1. vol. i. 2012. doi:10.1520/D2699-15A.

[2] ASTM Int. Standard Test Method for Motor Octane Number of Spark-Ignition Engine Fuel 1. vol. i. 2011. doi:10.1520/D2700-11.2.

[3] Smolenskii EA, Vlasova G V, Lapidus AL. A Study of the Structure–Octane Number Relationship for Hydrocarbons. Dokl Phys Chem 2004;397:145–9. doi:10.1023/B:DOPC.0000035400.72438.a8.

[4] Lapidus AL, Smolenskii EA, Bavykin VM, Myshenkova TN, Kondrat'ev LT. Models for the calculation and prediction of the octane and cetane numbers of individual hydrocarbons. Pet Chem 2008;48:277–86. doi:10.1134/S0965544108040051.

[5] Daly SR, Niemeyer KE, Cannella WJ, Hagen CL. Predicting fuel research octane number using Fourier-transform infrared absorption spectra of neat hydrocarbons. Fuel 2016;183:359–65. doi:10.1016/j.fuel.2016.06.097.

[6] Bassam A, Conde-Gutierrez RA, Castillo J, Laredo G, Hernandez JA. Direct neural network modeling for separation of linear and branched paraffins by adsorption process for gasoline octane number improvement. Fuel 2014;124:158–67. doi:10.1016/j.fuel.2014.01.080.

[7] AlRamadan AS, Sarathy SM, Khurshid M, Badra J. A blending rule for octane numbers of PRFs and TPRFs with ethanol. Fuel 2016;180:175–86. doi:10.1016/j.fuel.2016.04.032.

[8] Badra JA, Bokhumseen N, Mulla N, Sarathy SM, Farooq A, Kalghatgi G, et al. A methodology to relate octane numbers of binary and ternary n-heptane, iso-octane and toluene mixtures with simulated ignition delay times. Fuel 2015;160:458–69. doi:10.1016/j.fuel.2015.08.007.

[9] Kalghatgi G, Babiker H, Badra J. A Simple Method to Predict Knock Using Toluene, N-Heptane and Iso-Octane Blends (TPRF) as Gasoline Surrogates. SAE Int J Engines 2015;8:2015-01–0757. doi:10.4271/2015-01-0757.

[10] Morgan N, Smallbone A, Bhave A, Kraft M, Cracknell R, Kalghatgi G. Mapping surrogate gasoline compositions into RON/MON space. Combust Flame 2010;157:1122–31. doi:10.1016/j.combustflame.2010.02.003.

[11] Yuan H, Yang Y, Brear MJ, Foong TM, Anderson JE. Optimal octane number correlations for mixtures of toluene reference fuels (TRFs) and ethanol. Fuel 2017;188:408–17. doi:10.1016/j.fuel.2016.10.042.
[12] Meusinger R, Moros R. Determination of octane numbers of gasoline compounds from their chemical structure by 13 C NMR spectroscopy and neural networks 2001;80.
[13] Andrade JM, Muniategui S, Prada D. Prediction of clean octane numbers of catalytic reformed naphthas using FT-m.i.r. and PLS. Fuel 1997;76:1035–42. doi:10.1016/S0016-2361(97)00095-1.
[14] Lugo HJ, Ragone G, Zambrano J. Correlations between Octane Numbers and Catalytic Cracking Naphtha Composition. Ind Eng Chem Res 1999;38:2171–6. doi:10.1021/ie980273r.
[15] Mendes G, Aleme HG, Barbeira PJS. Determination of octane numbers in gasoline by distillation curves and partial least squares regression. Fuel 2012;97:131–6. doi:10.1016/j.fuel.2012.01.058.
[16] Kamari A, Sattari M, Mohammadi AH, Ramjugernath D. Modeling of the Properties of Gasoline and Petroleum Fractions Using a Robust Scheme. Pet Sci Technol 2015;33:639–48. doi:10.1080/10916466.2014.999940.
[17] Nikolaou N, Papadopoulos CE, Gaglias IA, Pitarakis KG. A new non-linear calculation method of isomerisation gasoline research octane number based on gas chromatographic data. Fuel 2004;83:517–23. doi:10.1016/j.fuel.2003.09.011.
[18] Guan L, Feng XL, Li ZC, Lin GM. Determination of octane numbers for clean gasoline using dielectric spectroscopy. Fuel 2009;88:1453–9. doi:10.1016/j.fuel.2009.02.017.
[19] Flecher PE, Welch WT, Albin S, Cooper JB. Determination of octane numbers and Reid vapor pressure in commercial gasoline using dispersive fiber-optic Raman spectroscopy. Spectrochim Acta Part A Mol Biomol Spectrosc 1997;53A:199–206. doi:10.1016/S1386-1425(97)83026-0.
[20] Maylin MV, Kirgina MV, Sviridova EV, Sakhnevitch BV, Ivanchina ED. Calculation of Gasoline Octane Numbers Taking into Account the Reaction Interaction of Blend Components. Procedia Chem 2014;10:477–84. doi:10.1016/j.proche.2014.10.080.
[21] Teixeira LSG, Dantas MSG, Guimarães PRB, Teixeira W, Vargas H, Lima JAP. Correlation of PVR, Octane Numbers and Distillation Curve of Gasoline with Data from a Thermal Wave Interferometer. Comput. Aided Chem. Eng., vol. 27, 2009, p. 759–64. doi:10.1016/S1570-7946(09)70347-5.
[22] Naser N, Yang SY, Kalghatgi G, Chung SH. Relating the octane numbers of fuels to ignition delay times measured in an ignition quality tester (IQT). Fuel 2017;187:117–27. doi:10.1016/j.fuel.2016.09.013.
[23] Abdul Jameel AG, Sarathy SM. Prediction of RON and MON of gasoline-ethanol using 1 H NMR spectroscopy. Proc. Eur. Combust. Meet. 2017, n.d.
[24] Foong TM, Morganti KJ, Brear MJ, da Silva G, Yang Y, Dryer FL. The octane numbers of ethanol blended with gasoline and its surrogates. Fuel 2014;115:727–39. doi:10.1016/j.fuel.2013.07.105.
[25] Anderson JE, Leone TG, Shelby MH, Wallington TJ, Bizub JJ, Foster M, et al. Octane Numbers of Ethanol-Gasoline Blends: Measurements and Novel Estimation Method from Molar Composition. SAE Tech. Pap., 2012, p. 133. doi:10.4271/2012-01-1274.
[26] Badra J, AlRamadan AS, Sarathy SM. Optimization of the octane response of gasoline/ethanol blends. Appl Energy 2017;203:778–93.

doi:10.1016/j.apenergy.2017.06.084.
[27] Corsetti S, Zehentbauer FM, McGloin D, Kiefer J. Characterization of gasoline/ethanol blends by infrared and excess infrared spectroscopy. Fuel 2015;141:136–42. doi:10.1016/j.fuel.2014.10.025.
[28] Abdul Jameel AG, Han Y, Brignoli O, Telalović S, Elbaz AM, Im HG, et al. Heavy fuel oil pyrolysis and combustion: Kinetics and evolved gases investigated by TGA-FTIR. J Anal Appl Pyrolysis 2017. doi:10.1016/j.jaap.2017.08.008.
[29] Palani R, AbdulGani A, Balasubramanian N. Treatment of Tannery Effluent Using a Rotating Disc Electrochemical Reactor. Water Environ Res 2017;89:77–85. doi:10.2175/106143016X14609975746046.
[30] de Paulo JM, Barros JEM, Barbeira PJS. A PLS regression model using flame spectroscopy emission for determination of octane numbers in gasoline. Fuel 2016;176:216–21. doi:10.1016/j.fuel.2016.02.033.
[31] Abdul Jameel AG, Sarathy SM. Lube Products: Molecular Characterization of Base Oils. Encycl. Anal. Chem., Chichester, UK: John Wiley & Sons, Ltd; 2018, p. 1–14. doi:10.1002/9780470027318.a1824.pub2.
[32] Abdul Jameel AG, Elbaz AM, Emwas A-H, Roberts WL, Sarathy SM. Calculation of Average Molecular Parameters, Functional Groups, and a Surrogate Molecule for Heavy Fuel Oils Using 1 H and 13 C Nuclear Magnetic Resonance Spectroscopy. Energy & Fuels 2016;30:3894–905. doi:10.1021/acs.energyfuels.6b00303.
[33] Elfghi FM. A hybrid statistical approach for modeling and optimization of RON: A comparative study and combined application of response surface methodology (RSM) and artificial neural network (ANN) based on design of experiment (DOE). Chem Eng Res Des 2016;113:264–72. doi:10.1016/j.cherd.2016.05.023.
[34] Murty BS., Rao R. Global optimization for prediction of blend composition of gasolines of desired octane number and properties. Fuel Process Technol 2004;85:1595–602. doi:10.1016/j.fuproc.2003.08.004.
[35] Pasadakis N, Gaganis V, Foteinopoulos C. Octane number prediction for gasoline blends. Fuel Process Technol 2006;87:505–9. doi:10.1016/j.fuproc.2005.11.006.
[36] Yahyaoui M, Djebaïli-Chaumeix N, Dagaut P, Paillard C-E, Gail S. Experimental and modelling study of gasoline surrogate mixtures oxidation in jet stirred reactor and shock tube. Proc Combust Inst 2007;31:385–91. doi:10.1016/j.proci.2006.07.179.
[37] Abdul Jameel AG, Naser N, Emwas A-H, Dooley S, Sarathy SM. Predicting Fuel Ignition Quality Using 1 H NMR Spectroscopy and Multiple Linear Regression. Energy & Fuels 2016;30:9819–35. doi:10.1021/acs.energyfuels.6b01690.
[38] Dahmen M, Marquardt W. A Novel Group Contribution Method for the Prediction of the Derived Cetane Number of Oxygenated Hydrocarbons. Energy & Fuels 2015;29:5781–801. doi:10.1021/acs.energyfuels.5b01032.
[39] Barrientos EJ, Lapuerta M, Boehman AL. Group additivity in soot formation for the example of C-5 oxygenated hydrocarbon fuels. Combust Flame 2013;160:1484–98. doi:10.1016/j.combustflame.2013.02.024.
[40] Yang Y, Boehman AL, Santoro RJ. A study of jet fuel sooting tendency using the threshold sooting index (TSI) model. Combust Flame 2007;149:191–205. doi:10.1016/j.combustflame.2006.11.007.
[41] Kumar K, Sung C-J. Flame Propagation and Extinction Characteristics of Neat Surrogate Fuel Components. Energy & Fuels 2010;24:3840–9. doi:10.1021/ef100074v.

[42] Hechinger M, Marquardt W. Targeted QSPR for the prediction of the laminar burning velocity of biofuels. Comput Chem Eng 2010;34:1507–14. doi:10.1016/j.compchemeng.2010.02.022.
[43] Saldana DA, Starck L, Mougin P, Rousseau B, Pidol L, Jeuland N, et al. Flash Point and Cetane Number Predictions for Fuel Compounds Using Quantitative Structure Property Relationship (QSPR) Methods. Energy & Fuels 2011;25:3900–8. doi:10.1021/ef200795j.
[44] Abdul Jameel AG, Naser N, Issayev G, Touitou J, Ghosh MK, Emwas A, et al. A minimalist functional group (MFG) approach for surrogate fuel formulation. Combust Flame 2018;192:250–71. doi:10.1016/j.combustflame.2018.01.036.
[45] Abdul Jameel AG, Naser N, Emwas A-H, Sarathy SM. Surrogate formulation for diesel and jet fuels using the minimalist functional group (MFG) approach. Proc Combust Inst 2018.
[46] Rao VK, Bardon MF. Estimating the molecular weight of petroleum fractions. Ind Eng Chem Process Des Dev 1985;24:498–500. doi:10.1021/i200029a046.
[47] Santamaría A, Mondragón F, Quiñónez W, Eddings EG, Sarofim AF. Average structural analysis of the extractable material of young soot gathered in an ethylene inverse diffusion flame. Fuel 2007;86:1908–17. doi:10.1016/j.fuel.2006.12.002.
[48] Hauser A, AlHumaidan F, Al-Rabiah H, Halabi MA. Study on Thermal Cracking of Kuwaiti Heavy Oil (Vacuum Residue) and Its SARA Fractions by NMR Spectroscopy. Energy & Fuels 2014;28:4321–32. doi:10.1021/ef401476j.
[49] Bebis G, Georgiopoulos M. Feed-forward neural networks. IEEE Potentials 1994;13:27–31. doi:10.1109/45.329294.
[50] Sarathy SM, Farooq A, Kalghatgi GT. Recent progress in gasoline surrogate fuels. Prog Energy Combust Sci 2018;65:67–108. doi:10.1016/j.pecs.2017.09.004.
[51] Lapuerta M, Hernández JJ, Sarathy SM. Effects of methyl substitution on the auto-ignition of C16 alkanes. Combust Flame 2016;164:259–69. doi:10.1016/j.combustflame.2015.11.024.
[52] Sarathy SM, Kukkadapu G, Mehl M, Wang W, Javed T, Park S, et al. Ignition of alkane-rich FACE gasoline fuels and their surrogate mixtures. Proc Combust Inst 2015;35:249–57. doi:10.1016/j.proci.2014.05.122.
[53] Won SH, Dooley S, Veloo PS, Wang H, Oehlschlaeger MA, Dryer FL, et al. The combustion properties of 2,6,10-trimethyl dodecane and a chemical functional group analysis. Combust Flame 2014;161:826–34. doi:10.1016/j.combustflame.2013.08.010.
[54] Dussan K, Dooley S, Dryer FL, Won SH. A Nuclear Magnetic Resonance Orientated Combustion Property Regression. 9th U S Natl Combust Meet 2015.
[55] Sarathy SM, Javed T, Karsenty F, Heufer A, Wang W, Park S, et al. A comprehensive combustion chemistry study of 2,5-dimethylhexane. Combust Flame 2014;161:1444–59. doi:10.1016/j.combustflame.2013.12.010.
[56] Karsenty F, Sarathy SM, Togbé C, Westbrook CK, Dayma G, Dagaut P, et al. Experimental and Kinetic Modeling Study of 3-Methylheptane in a Jet-Stirred Reactor. Energy & Fuels 2012;26:4680–9. doi:10.1021/ef300852w.
[57] Mani Sarathy S, Niemann U, Yeung C, Gehmlich R, Westbrook CK, Plomer M, et al. A counterflow diffusion flame study of branched octane isomers. Proc Combust Inst 2013;34:1015–23. doi:10.1016/j.proci.2012.05.106.
[58] Wang W, Li Z, Oehlschlaeger MA, Healy D, Curran HJ, Sarathy SM, et al. An experimental and modeling study of the autoignition of 3-methylheptane. Proc Combust

Inst 2013;34:335–43. doi:10.1016/j.proci.2012.06.001.
[59] Mohamed SY, Cai L, Khaled F, Banyon C, Wang Z, Al Rashidi MJ, et al. Modeling Ignition of a Heptane Isomer: Improved Thermodynamics, Reaction Pathways, Kinetics, and Rate Rule Optimizations for 2-Methylhexane. J Phys Chem A 2016;120:2201–17. doi:10.1021/acs.jpca.6b00907.
[60] Al MJ, Mehl M, Pitz WJ, Mohamed S, Sarathy SM. Cyclopentane combustion chemistry . Part I : Mechanism development and computational kinetics. Combust Flame 2017;183:358–71. doi:10.1016/j.combustflame.2017.05.018.
[61] Al MJ, Mármol JC, Banyon C, Sajid MB, Mehl M, Pitz WJ, et al. Cyclopentane combustion . Part II . Ignition delay measurements and mechanism validation. Combust Flame 2017;183:372–85. doi:10.1016/j.combustflame.2017.05.017.
[62] Sarathy SM, Oßwald P, Hansen N, Kohse-Höinghaus K. Alcohol combustion chemistry. Prog Energy Combust Sci 2014;44:40–102. doi:10.1016/j.pecs.2014.04.003.
[63] Waqas MU, Atef N, Singh E, MASURIER J-B, Sarathy M, Johansson B. Blending Behavior of Ethanol with PRF 84 and FACE A Gasoline in HCCI Combustion Mmode, 2017. doi:10.4271/2017-24-0082.
[64] Kapur GS, Ecker A, Meusinger R. Establishing Quantitative Structure−Property Relationships (QSPR) of Diesel Samples by Proton-NMR & Multiple Linear Regression (MLR) Analysis. Energy & Fuels 2001;15:943–8. doi:10.1021/ef010021u.
[65] Vatani A, Mehrpooya M, Gharagheizi F. Prediction of Standard Enthalpy of Formation by a QSPR Model. Int J Mol Sci 2007;8:407–32. doi:10.3390/i8050407.
[66] Geng P, Conran D. Correlation of Chemical Compositions and Fuel Properties with Fuel Octane Rating of Gasoline Containing Ethanol. SAE Pap., 2011, p. 1310–20. doi:10.4271/2011-01-1986.
[67] Zhou Z, Yang Y, Brear M, Lacey J, Leone TG, Anderson JE, et al. A Comparison of Four Methods for Determining the Octane Index and K on a Modern Engine with Upstream, Port or Direct Injection. SAE Tech. Pap., 2017. doi:10.4271/2017-01-0666.
[68] Cloudflame webpage n.d.
[69] Goteng GL, Nettyam N, Sarathy SM. CloudFlame: Cyberinfrastructure for Combustion Research. 2013 Int. Conf. Inf. Sci. Cloud Comput. Companion, IEEE; 2013, p. 294–9. doi:10.1109/ISCC-C.2013.57.
[70] Flynn JH, Wall LA. Knocking Characteristics of Pure Hydrocarbons. vol. 70A. 100 Barr Harbor Drive, PO Box C700, West Conshohocken, PA 19428-2959: ASTM International; 1958. doi:10.1520/STP225-EB.
[71] Solaka H, Tuner M, Johansson B, Cannella W. Gasoline Surrogate Fuels for Partially Premixed Combustion, of Toluene Ethanol Reference Fuels, 2013. doi:10.4271/2013-01-2540.
[72] Singh E, Badra J, Mehl M, Sarathy SM. Chemical Kinetic Insights into the Octane Number and Octane Sensitivity of Gasoline Surrogate Mixtures. Energy & Fuels 2017;31:1945–60. doi:10.1021/acs.energyfuels.6b02659.

Table 1

^{1}H NMR assignments of the functional groups

Chemical shift region (ppm)	H type	Integral intensity
6.42 – 8.99	aromatics	A
4.50 – 6.42	olefinic CH and CH_2 groups	B
2.88 – 3.40	α-CH	C
2.64 – 2.88	α-CH_2	D
2.04 – 2.64	α-CH_3	E
1.57 – 1.96	naphthenic CH and CH_2 groups	F
1.39 – 1.57	paraffinic CH groups	G
0.94 – 1.39	paraffinic CH_2 groups	H
0.25 – 0.94	paraffinic CH_3 groups	I
3.68 – 3.78	ethanolic OH groups	OH
	Total (A+B+C+D+E+F+G+H+I+OH)	T
0.84 – 0.87	paraffinic CH_3 groups connected to the longest chain towards the interior	J
1.35 – 1.39	paraffinic CH_2 groups connected to the longest chain towards the interior	K
2.31 – 2.34	α-CH_3 groups in the meta position with respect to other α-CH_3 groups	L
2.17 – 2.19	α-CH_3 groups in the para position with respect to other α-CH_3 groups	M

Table 2

Formulas used to calculate the weight % of the functional groups

Functional groups	H type (mol %)	Weight (arb.unit)	Weight (%)
Paraffinic CH_3	$M_{P_{CH_3}} = \frac{(I+E)}{T} * 100$	$G_{P_{CH_3}} = \frac{M_{P_{CH_3}} * 15}{3}$	$W_{P_{CH_3}} = \frac{G_{P_{CH_3}} * 100}{G_{P_{CH_3}} + G_{P_{CH_2}} + G_{P_{CH}} + G_{O_{CH.CH_2}} + G_{N_{CH.CH_2}} + G_{A_{C.CH}} + G_{OH}}$
Paraffinic CH_2	$M_{P_{CH_2}} = \frac{(H+D)}{T} * 100$	$G_{P_{CH_2}} = \frac{M_{P_{CH_2}} * 14}{2}$	$W_{P_{CH_2}} = \frac{G_{P_{CH_2}} * 100}{G_{P_{CH_3}} + G_{P_{CH_2}} + G_{P_{CH}} + G_{O_{CH.CH_2}} + G_{N_{CH.CH_2}} + G_{A_{C.CH}} + G_{OH}}$
Paraffinic CH	$M_{P_{CH}} = \frac{(G+C)}{T} * 100$	$G_{P_{CH}} = \frac{M_{P_{CH}} * 13}{1}$	$W_{P_{CH}} = \frac{G_{P_{CH}} * 100}{G_{P_{CH_3}} + G_{P_{CH_2}} + G_{P_{CH}} + G_{O_{CH.CH_2}} + G_{N_{CH.CH_2}} + G_{A_{C.CH}} + G_{OH}}$
Olefinic CH-CH_2	$M_{O_{CH.CH_2}} = \frac{B}{T} * 100$	$G_{O_{CH.CH_2}} = \frac{M_{O_{CH.CH_2}} * 13.5}{1.5}$	$W_{O_{CH.CH_2}} = \frac{G_{O_{CH.CH_2}} * 100}{G_{P_{CH_3}} + G_{P_{CH_2}} + G_{P_{CH}} + G_{O_{CH.CH_2}} + G_{N_{CH.CH_2}} + G_{A_{C.CH}} + G_{OH}}$
Naphthenic CH-CH_2	$M_{N_{CH.CH_2}} = \frac{F}{T} * 100$	$G_{N_{CH.CH_2}} = \frac{M_{N_{CH.CH_2}} * 13.5}{1.5}$	$W_{N_{CH.CH_2}} = \frac{G_{N_{CH.CH_2}} * 100}{G_{P_{CH_3}} + G_{P_{CH_2}} + G_{P_{CH}} + G_{O_{CH.CH_2}} + G_{N_{CH.CH_2}} + G_{A_{C.CH}} + G_{OH}}$
α-CH	$M_{\alpha-\mathrm{CH}} = \frac{C}{T} * 100$		
α-CH_2	$M_{\alpha-\mathrm{CH_2}} = \frac{D}{T} * 100$		
α-CH_3	$M_{\alpha-\mathrm{CH_3}} = \frac{E}{T} * 100$		
Aromatic C-CH	$M_{A_{C.CH}} = \frac{A}{T} * 100$	$G_{A_{C.CH}} = \frac{M_{A_{C.CH}} * 13}{1} + \frac{M_{\alpha-\mathrm{CH}} * 13}{1} + \frac{M_{\alpha-\mathrm{CH_2}} * 14}{2} + \frac{M_{\alpha-\mathrm{CH_3}} * 15}{3}$	$W_{A_{C.CH}} = \frac{G_{A_{C.CH}} * 100}{G_{P_{CH_3}} + G_{P_{CH_2}} + G_{P_{CH}} + G_{O_{CH.CH_2}} + G_{N_{CH.CH_2}} + G_{A_{C.CH}} + G_{OH}}$
Ethanolic OH	$M_{OH} = \frac{OH}{T} * 100$	$G_{OH} = \frac{M_{OH} * 17}{1}$	$W_{OH} = \frac{G_{OH} * 100}{G_{P_{CH_3}} + G_{P_{CH_2}} + G_{P_{CH}} + G_{O_{CH.CH_2}} + G_{N_{CH.CH_2}} + G_{A_{C.CH}} + G_{OH}}$

Table 3

RON and MON of pure hydrocarbons. Ref [70]

S. No.	Name	RON	MON
1	Propane	112	97.1
2	n-butane	93.8	89.6
3	n-pentane	61.7	62.6
4	2-methylpentane	73.4	73.5
5	3-methylpentane	74.5	74.3
6	2,2-dimethylbutane	91.8	93.4
7	2,3-dimethylbutane	100.3	94.3
8	3-ethylpentane	65	69.3
9	2,2-dimethylpentane	92.8	95.6
10	2,3-dimethylpentane	91.1	88.5
11	2,4-dimethylpentane	83.1	83.8
12	3,3-dimetmylpentane	80.8	86.6
13	2,2-dimethylhexane	72.5	77.4
14	2,3-dimethylhexane	73.4	78.9
15	2,4-dimethylhexane	65.2	69.9
16	3,3-dimethylhexane	75.5	83.4
17	3,4-dimethylhexane	76.3	81.7
18	2-methyl-3-ethylpentane	87.3	88.1
19	3-methyl-3-ethylpentane	80.8	88.7
20	2,2,3-trimethylpentane	101.2	99.9
21	2,2,4-trimethylpentane	100	100
22	2,3,3-trimethylpentane	100.6	99.4
23	2,3,4-trimethylpentane	100.2	95.9
24	3,3-diethylpentane	84	91.6
25	2,2-dimethyl-3-ethylpentane	101.8	99.5
26	2,4-dimethyl-3-ethylpentane	100.5	96.6
27	2,2,3,3-tetramethylpentane	103.6	95
28	3,3,5-trimethylheptane	86.4	88.7
29	2,2,3,3-tetramethylhexane	102	92.4
30	ethylene	100	75.6
31	propylene	100.2	84.9
32	1-butene	97.4	80.8
33	2-butene	100	83.5
34	1-pentene	90.9	77.1
35	2-methyl-1-butene	100.2	81.9
36	2-methyl-2-butene	97.3	84.7
37	1-hexene	76.4	63.4
38	2-methyl-1-pentene	94.2	81.5
39	3-methyl-1-pentene	96	81.2
40	4-methyl-1-pentene	95.7	80.9
41	2-methyl-2-pentene	97.8	83
42	4-methyl-2-pentene	99.7	84.5
43	2-ethyl-1-butene	98.3	79.4

44	2,3-dimethyl-1-butene	100.1	82.8
45	3,3-dimethyl-1-butene	101.7	93.3
46	2,3-dimethyl-2-butene	97.4	80.5
47	1-heptene	54.5	50.7
48	2-methyl-1-hexene	90.7	78.8
49	3-methyl-1-hexene	82.2	71.5
50	4-methyl-1-hexene	86.4	74
51	5-methyl-1-hexene	75.5	64
52	2-methyl-2-hexene	91.6	79.2
53	cis-3-methyl-2-hexene	92.4	80
54	3-ethyl-1-pentene	95.6	81.6
55	3-ethyl-2-pentene	93.7	80.6
56	2,3-dimethyl-1-pentene	99.3	84.2
57	2,4-dimethyl-1-pentene	99.2	84.6
58	3,3-dimethyl-1-pentene	100.3	86.1
59	3,4-dimethyl-1-pentene	98.9	80.9
60	4,4-dimethyl-1-pentene	100.4	85.4
61	2,3-dimethyl-2-pentene	97.5	80
62	2,4-dimethyl-2-pentene	100	85.3
63	cis-3,4-dimethyl-2-pentene	96	82.2
64	cis-4,4-dimethyl-2-pentene	100.5	90.2
65	3-methyl-2-ethyl-1-buteme	97	82
66	2,3,3-trimethyl-1-butene	100.5	90.5
67	2-methyl-1-heptene	70.2	66.3
68	2,3-dimethyl-1-hexene	96.3	83.6
69	2,3-dimethyl-2-hexene	93.1	79.3
70	cis-2,2-dimethyl-3-hexene	100.7	88
71	2,3,3-trimethyl-1-pentene	100.6	85.7
72	2,4,4-trimethyl-1-pentene	100.6	86.5
73	2,4,4-trimethyl-2-pentene	100.3	86.2
74	2-methyl-1,3-butadiene	99.1	81
75	1,5-hexadiene	71.1	37.6
76	cyclopentene	93.3	69.7
77	1-methyl-cyclopentene	93.6	72.9
78	1-ethylcyclopentene	90.3	72
79	3-ethylcyclopentene	90.8	71.4
80	cyclohexene	83.9	63
81	1-methylcyclohexene	89.2	72
82	1-ethylcyclohexene	85	70.5
83	cyclopentane	100.1	84.9
84	methylcyclopentane	91.3	80
85	ethylcyclopentane	67.2	61.2
86	1,1-dimethylcyclopentane	92.3	89.3
87	1,3-dimethylcyclopentane	79.2	73.1
88	n-propylcyclopentane	31.2	28.1
89	isopropylcyclopentane	81.1	76.2
90	1-methyl-3-ethyl-ccyclopentane	57.6	59.8
91	1,1,3-trimetmylcyclopentane	87.7	83.5

92	cyclohexane	83	77.2
93	methylcyclohexane	74.8	71.1
94	ethylcyclohexane	45.6	40.8
95	1,1-dimethylcyclohexane	87.3	85.9
96	1,2-dimethylcyclohexane	80.9	78.6
97	i,3-dimetmylcyclohexane	71.7	71
98	i,4-dimethylcyclohexane	67.2	68.2
99	isopropylcyclohexane	62.8	61.1
100	benzene	105	102.8
101	toluene	118	100.3
102	ethylbenzene	100.8	97.9
103	o-xylene	105	100
104	m-xylene	104	102.8
105	p-xylene	103.4	101.2
106	n-propylbenzene	101.5	98.7
107	isopropylbenzene	102.1	99.3
108	o-ethyltoluene	100.2	92.1
109	m-ethyltoluene	101.8	100
110	p-ethyltoluene	102	97
111	1,2,3-trimethylbenzene	100.5	101.1
112	1,3,5-trimethylbenzene	106	100.6
113	n-butylbenzene	100.4	94.5
114	isobutylbenzene	101.6	98
115	sec-butylbenzene	100.7	95.7
116	tert-butylbenzene	103	100.8
117	1-methyl-2-n-propylbenzene	100.3	92.2
118	1-methyl-3-n-propylbenzene	101.8	100
119	o-cymene	100.6	96
120	p-cynene	101.4	97.7
121	m-diethylbenzene	103	97
122	p-diethylbenzene	100.6	95.2
123	1,2-dimethyl-3-ethylbenzene	100.4	91.9
124	1,3-dimethyl-4-ethylbenzene	100.6	95.9
125	1,3-dimethyl-5-ethylbenzene	102.7	100.2
126	1,4-dimethyl-2-ethylbenzene	100.6	96
127	1,2,3,4-tetramethylbenzene	100.5	100
128	ethanol	108[a]	90[a]

a:taken from [7]

Table 4

RON and MON of hydrocarbon blends

S.no	Name	Components (vol %)							RON	MON	Ref
		n-heptane	i-octane	toluene	TMB	CP	1-hexene	ethanol			
1	PRF+10	54	36					10	55.6	53	[7]
2	PRF+20	48	32					20	69	64	[7]
3	PRF+30	42	28					30	80.7	76	[7]
4	PRF+40	36	24					40	90.5	83.6	[7]
5	PRF+50	30	20					50	97.9	87.5	[7]
6	PRF+60	24	16					60	102.5	89	[7]
7	PRF+70	18	12					70	104.8	89.8	[7]
8	PRF+80	12	8					80	105.3	90.2	[7]
9	PRF+90	6	4					90	108.5	91	[7]
10	TPRF 1+0	42.5	47.3	10.2				0	60.8	58	[7]
11	TPRF 1+10	38.3	42.5	9.2				10	71.9	68	[7]
12	TPRF 1+20	34.0	37.8	8.2				20	82.5	77.7	[7]
13	TPRF 1+40	25.5	28.4	6.1				40	97.8	87.8	[7]
14	TPRF 1+60	17.0	18.9	4.1				60	105.2	88.5	[7]
15	TPRF 2+0	46.5	33.7	19.8				0	59.5	55.5	[7]
16	TPRF 2+10	41.9	30.3	17.8				10	70.3	65	[7]
17	TPRF 2+20	37.2	27.0	15.8				20	81	75.8	[7]
18	TPRF 2+40	27.9	20.2	11.9				40	96.8	86.6	[7]
19	TPRF 2+60	18.6	13.5	7.9				60	104.4	89.7	[7]
20	TPRF 3+0	54.2	5.6	40.2				0	57.5	50.7	[7]
21	TPRF 3+10	48.8	5.0	36.2				10	68.7	59.4	[7]
21	TPRF 3+20	43.3	4.5	32.2				20	78.3	70.5	[7]
23	TPRF 3+40	32.5	3.4	24.1				40	94.4	84.3	[7]
24	TPRF 3+60	21.7	2.2	16.1				60	103.4	88.4	[7]
25	TPRF 4+1	40	60	0				0	60.6	60.8	[71]
26	TPRF 4+2	40	45	15				0	64.3	62.3	[71]
27	TPRF 4+3	35	57.5	7.5				0	67.3	66.1	[71]
28	TPRF 4+4	40	47.5	7.5				5	66.6	64	[71]
29	TPRF 4+5	30	70	0				0	70.3	70.4	[71]
30	TPRF 4+6	40	35	15				10	72.2	69	[71]
31	TPRF 4+7	35	60	0				5	70.5	68.7	[71]
32	TPRF 4+8	30	55	15				0	74.2	71.9	[71]
33	TPRF 4+9	40	50	0				10	69.7	66.8	[71]
34	TPRF 4+10	35	45	15				5	73.5	69.4	[71]
35	TPRF 4+11	35	52.5	7.5				5	71.9	69.4	[71]
36	TPRF 4+12	35	47.5	7.5				10	74.9	71.8	[71]
37	TPRF 4+13	30	57.5	7.5				5	76.8	74.2	[71]
38	TPRF 4+14	30	60	0				10	78.7	76.7	[71]
39	TPRF 4+15	30	45	15				10	81.6	77.2	[71]
40	TMB+0				100			0	109.5	108	[26]
41	TMB+10				90			10	107	102	[26]
42	TMB+25				75			25	105	95.5	[26]
43	TMB+40				60			40	104	93.5	[26]
44	TMB+60				40			60	103.8	91	[26]
45	CP+0					100		0	100	85.6	[26]
46	CP+10					90		10	101	85.9	[26]

47	CP+25				75		25	102.3	86.3	[26]
48	CP+40				60		40	103.3	86.6	[26]
49	CP+60				40		60	104.8	87.2	[26]
50	Hex+0					100	0	73.6	64.5	[26]
51	Hex+10					90	10	81	68.5	[26]
52	Hex+25					75	25	89.2	74.5	[26]
53	Hex+40					60	40	96.5	79.5	[26]
54	Hex+60					40	60	101.7	84	[26]
55	TPRF 1	26.6	0.0	73.4				92.3	80.7	[72]
56	TPRF 2	9.8	72.3	17.9				93.7	90.3	[72]
57	TPRF 3	16.5	43.5	39.9				93	85.8	[72]
58	TPRF 4	14.6	51.7	33.7				93	86.7	[72]
59	TPRF 5	20.8	0.0	79.2				97.7	86.2	[72]
60	TPRF 6	10.0	65.1	24.9				95.2	90.5	[72]
61	TPRF 7	14.9	35.0	50.0				96.3	87.3	[72]
62	TPRF 8	16.6	69.3	14.1				86.6	84.2	[72]
63	TPRF 9	16.2	74.2	9.7				85.7	84.6	[72]
64	TPRF 10	13.7	42.8	43.5				96.3	88.3	[72]
65	TPRF 11	16.6	16.7	66.6				98	87.4	[72]
66	TPRF 12	66.6	16.7	16.7				39	37	[72]
67	TPRF 13	16.6	66.7	16.7				87	84	[72]
68	TPRF 14	49.9	0.0	50.1				65.9	57.7	[72]
69	TPRF 15	33.3	33.4	33.3				76.2	70.9	[72]
70	TPRF 16	41.9	0.0	58.1				75.6	66.9	[72]
71	TPRF 17	34.0	0.0	66.0				85.2	74.8	[72]
72	TPRF 18	30.0	0.0	70.0				89.3	78.2	[72]
73	TPRF 19	26.0	0.0	74.0				93.4	81.5	[72]
74	TPRF 20	21.0	5.0	73.9				96.9	85.2	[72]
75	TPRF 21	16.0	10.0	74.0				99.8	88.7	[72]
76	TPRF 22	36.0	54.0	10.0				66	64.4	[72]
77	TPRF 23	18.0	72.0	10.0				84.5	82	[72]
78	TPRF 24	32.0	48.0	20.0				73.6	70	[72]
79	TPRF 25	16.0	64.0	20.0				89.1	85.6	[72]
80	TPRF 26	56.0	14.0	30.0				53.2	48	[72]
81	TPRF 27	42.0	28.0	30.0				66.1	61	[72]
82	TPRF28	28.0	42.0	30.0				79	74	[72]
83	TPRF 29	14.0	56.0	30.0				92.8	86.9	[72]
84	TPRF 30	48.0	12.0	40.0				63.7	58	[72]
85	TPRF 31	36.0	24.0	40.0				75.1	68	[72]
86	TPRF 32	24.0	36.0	40.0				86.2	79.6	[72]
87	TPRF 33	11.9	48.0	40.0				96.7	88.7	[72]
88	TPRF 34	40.0	10.0	50.0				75.5	68	[72]
89	TPRF 35	30.0	20.0	50.0				83.8	76.2	[72]
90	TPRF 36	20.0	30.0	50.0				92.1	82.9	[72]
91	TPRF 37	9.9	40.0	50.0				99.8	90.9	[72]
92	TPRF 38	30.0	10.0	60.0				85.3	75.2	[72]
93	TPRF 39	20.0	20.0	60.0				95	83.7	[72]
94	TPRF 40	33.0	52.0	15.0				71.2	69	[72]
95	TPRF 41	40.0	30.0	30.0				68.4	63.7	[72]
96	TPRF 42	12.5	72.5	15.0				90.5	88	[72]
97	TPRF 43	17.5	52.5	30.0				89.5	84.7	[72]
98	MC 1	23.0	57.0	0.0		20.0		74.6	72	[72]
99	MC 2	31.0	44.0	15.0		10.0		72	68	[72]

100	MC 3	29.0	36.0	15.0		20.0	72	67.2	[72]
101	MC 4	5.1	84.7	0.0		10.2	92.9	90.2	[72]
102	MC 5	3.0	77.0	0.0		20.0	93	88.5	[72]
103	MC 6	10.0	65.0	15.0		10.0	91.2	86.8	[72]
104	MC 7	28.0	57.0	0.0	15.0		77.8	74.6	[72]
105	MC 8	7.0	58.0	15.0		20.0	91.7	85.2	[72]
106	MC 9	29.0	41.0	0.0	30.0		83	77.7	[72]
107	MC 10	14	46.5	32		7.5	91.4	84.9	[72]
108	MC 11	31.0	54.0	8.0	7.0		73.5	71.8	[72]
109	MC 12	11.0	39.0	30.0		20.0	90.9	82.7	[72]
110	MC 13	34.0	36.0	17.6	12.3		76.7	72	[72]
111	MC 14	9.0	76.0	0.0	15.0		94.2	90.5	[72]
112	MC 15	34.0	36.0	15.0	15.0		82.6	76.2	[72]
113	MC 16	9.0	61.0	0.0	30.0		96.8	90	[72]
114	MC 17	10.0	75.0	8.0	7.0		93.3	90.1	[72]
115	MC 18	12.5	57.5	15.0	15.0		94.4	88.4	[72]
116	MC 19	25.0	65.0	0.0		10.0	74.2	72.6	[72]
117	MC 20	9.0	81.0	0.0		10.0	94.1	91.4	[72]
118	MC 21	9.0	71.0	0.0		20.0	97.5	90.7	[72]
119	MC 22	13.0	62.0	15.0		10.0	93	88	[72]
120	MC 23	17.0	43.0	30.0		10.0	91.7	85.5	[72]
121	MC 24	14.0	51.0	15.0		20.0	94.5	87.8	[72]
122	MC 25	18.0	32.0	30.0		20.0	92.9	85.3	[72]
123	MC 26	43.0	7.0	30.0		20.0	70.9	66	[72]

i-octane refers to 2,2,4-trimethylpentane; TMB refers to 1,2,4-trimethylbenzene; CP refers to cyclopentane and MC refers to multi component;

Table 5

RON and MON of gasoline-ethanol blends. Ref [26]

S.no	Name	Components (vol %)							RON	MON
		FACE A gasoline	FACE C gasoline	FACE F gasoline	FACE G gasoline	FACE I gasoline	FACE F gasoline	ethanol		
1	FACE A+0	100						0	83.6	82.9
2	FACE A+10	90						10	92	88
3	FACE A+25	75						25	100.7	92.6
4	FACE A+40	60						40	104.1	91.7
5	FACE A+60	40						60	106	91.3
6	FACE C+0		100					0	84.4	83
7	FACE C+10		90					10	92.2	87.1
8	FACE C+25		75					25	100.3	90.5
9	FACE C+40		60					40	104.1	91
10	FACE C+60		40					60	105.8	91.3
11	FACE F+0			100				0	94.2	87.4
12	FACE F+10			90				10	98.9	88.5
13	FACE F+25			75				25	103.2	89.5
14	FACE F+40			60				40	104.7	90.3
15	FACE F+60			40				60	105.7	90.5
16	FACE G+0				100			0	96.4	84.9
17	FACE G+10				90			10	98.8	86.1
18	FACE G+25				75			25	102.4	87.9
19	FACE G+40				60			40	103	88.5
20	FACE G+60				40			60	105	88.9
21	FACE I+0					100		0	69.5	69
22	FACE I+10					90		10	79.9	78
23	FACE I+25					75		25	89.8	85.3
24	FACE I+40					60		40	98	88.3
25	FACE I+60					40		60	103.6	89.7
26	FACE J+0						100	0	71.8	66.9
27	FACE J+10						90	10	79	73.6
28	FACE J+25						75	25	89.8	81.7
29	FACE J+40						60	40	98	85.9
30	FACE J+60						40	60	103.6	88.2

Table 6

Final ANN architecture

ON	Architecture	Mean error		
		absolute	RMS	percentage
RON	9-540-314-1	1.6	2.2	1.8
MON	9-340-603-1	1.3	2.2	1.6

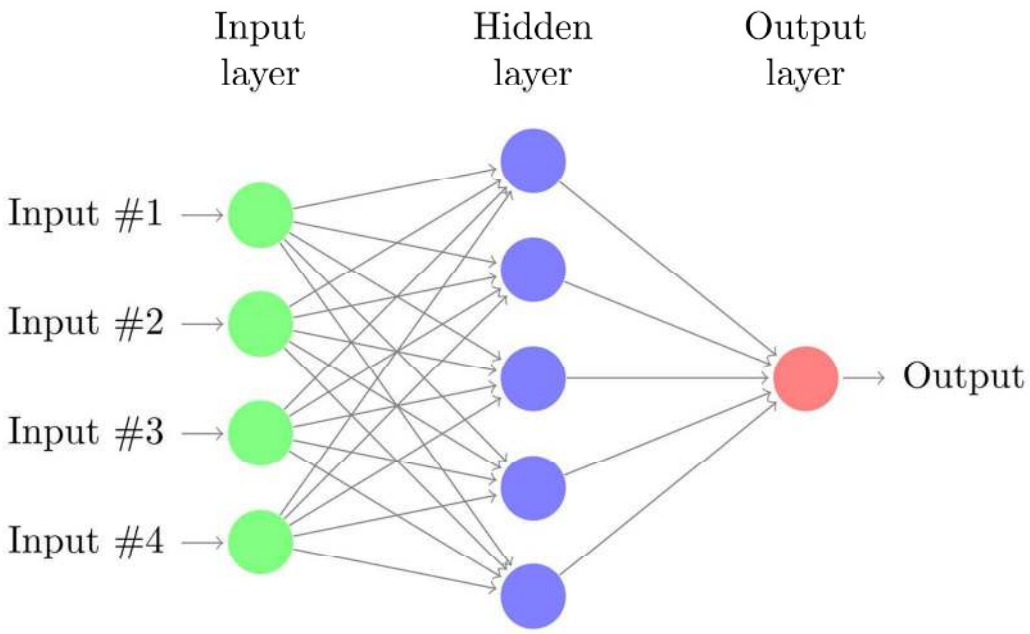

Figure 1. Overview of a simple neural network

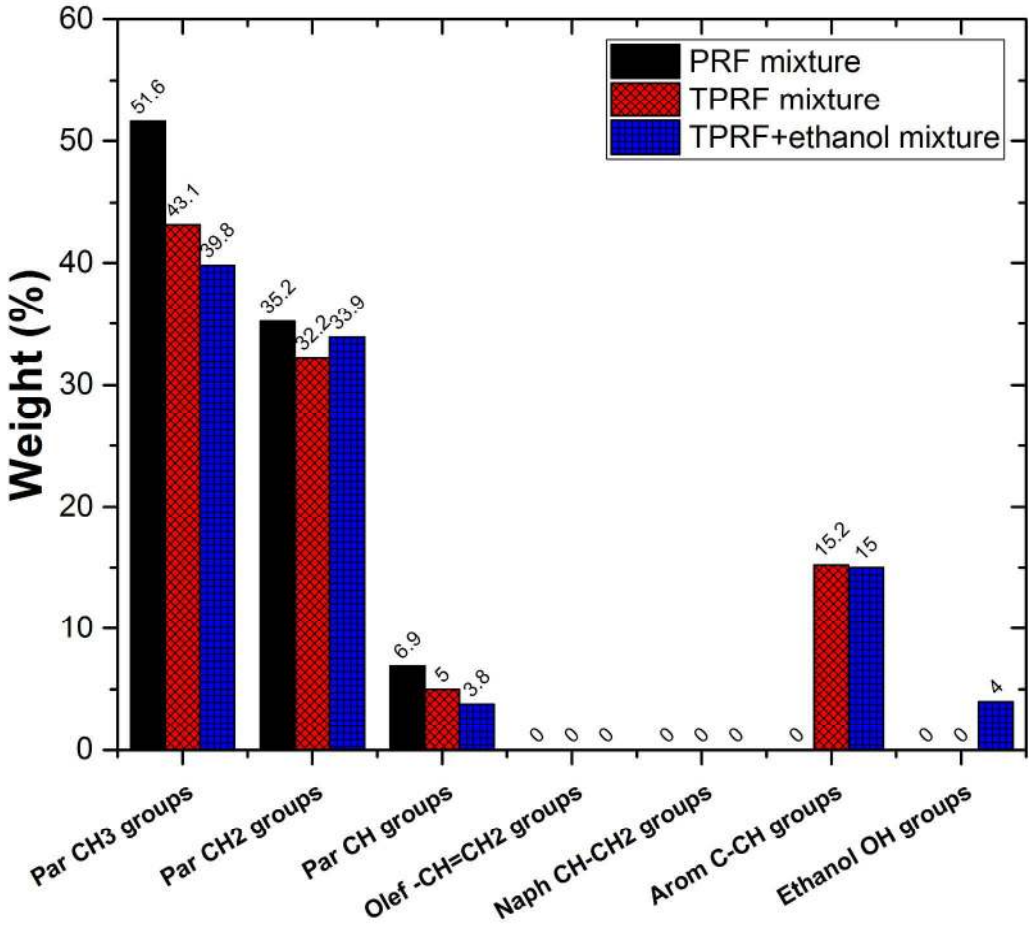

Figure 2. Functional groups present in three sample mixtures. Composition of each mixture is given in section 2.

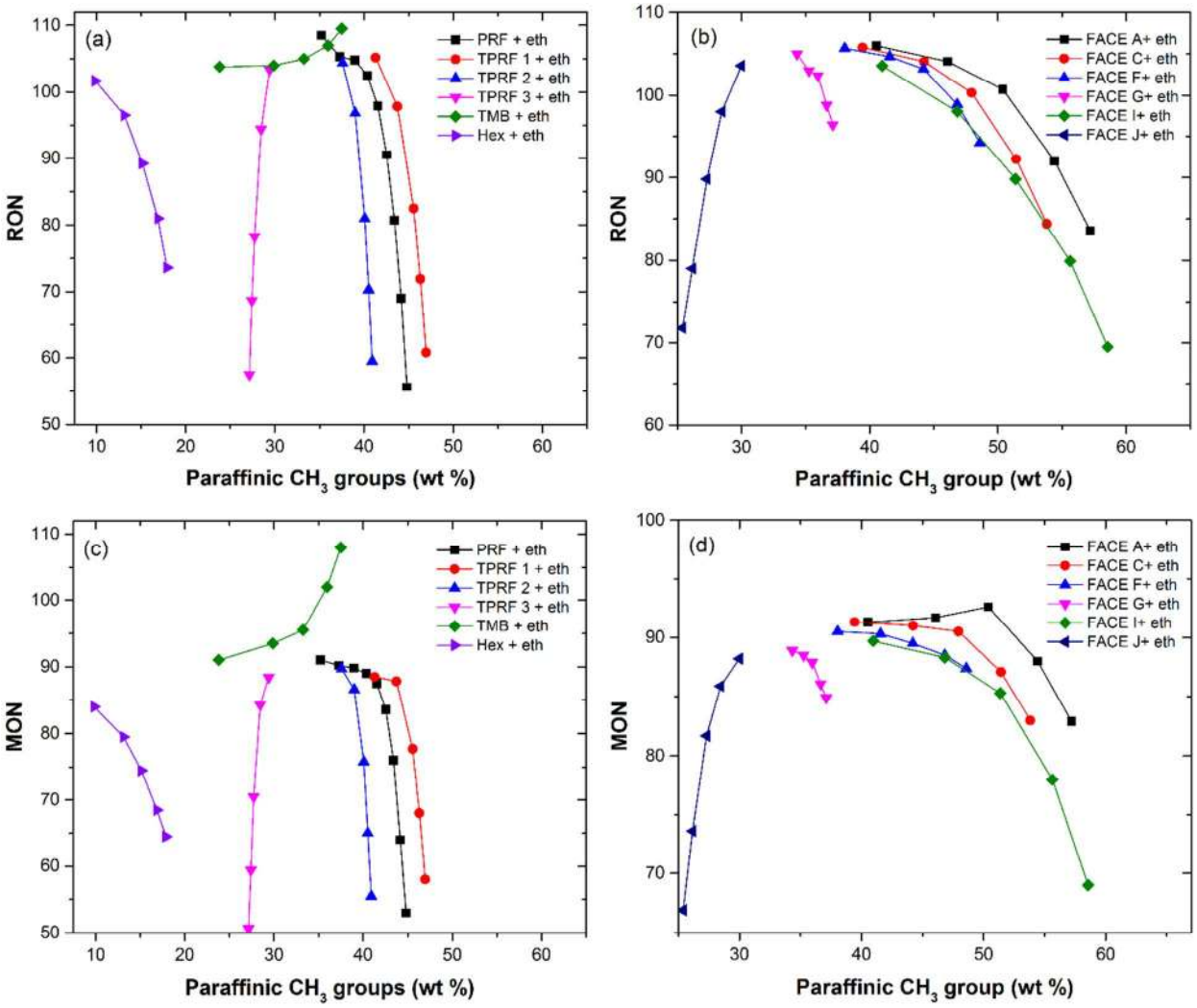

Figure 3. Effect of paraffinic CH_3 groups on a) RON of hydrocarbons blended with ethanol b) RON of FACE gasolines blended with ethanol c) MON of hydrocarbons blended with ethanol and d) MON of FACE gasolines blended with ethanol

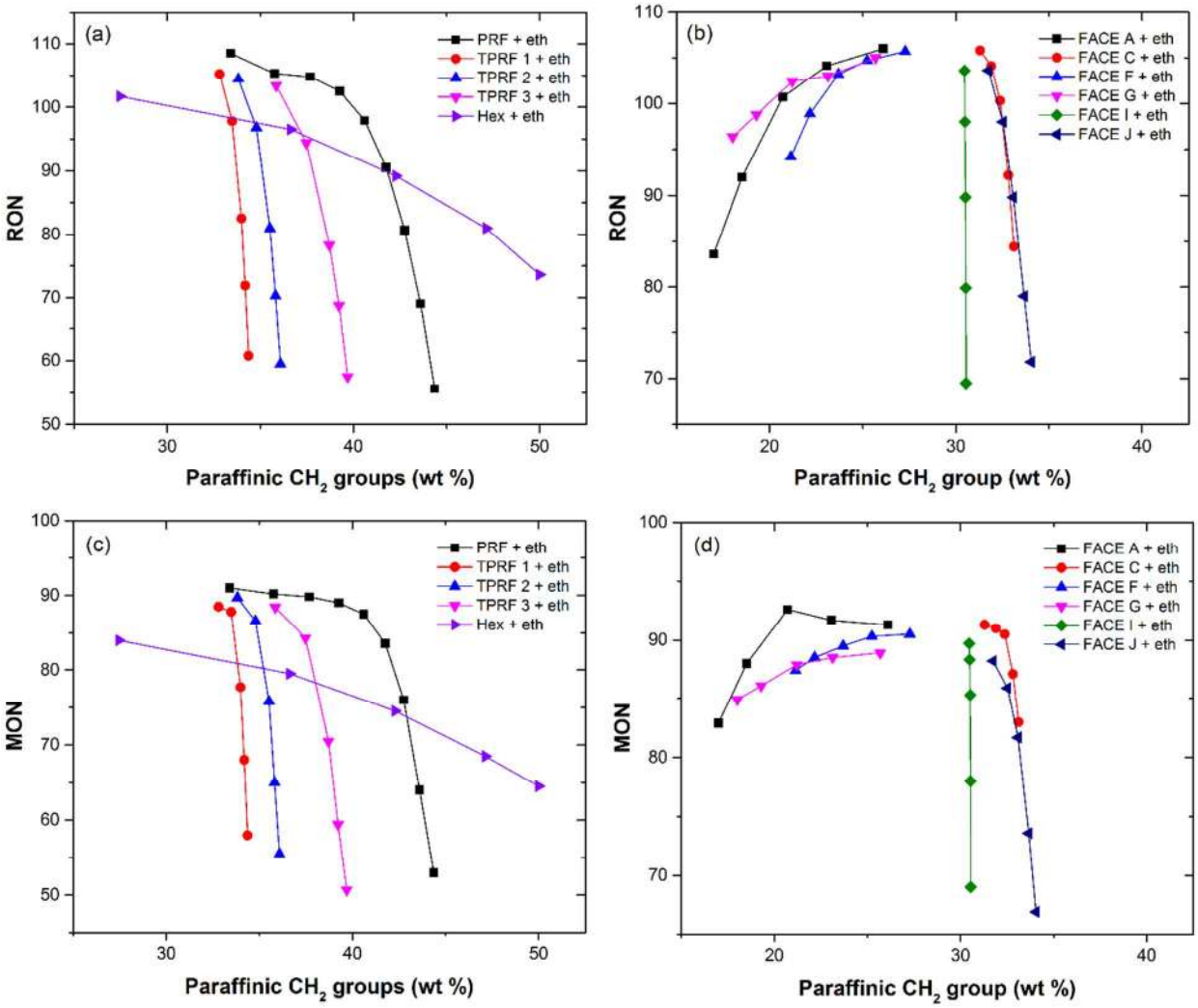

Figure 4. Effect of paraffinic CH_2 groups on a) RON of hydrocarbons blended with ethanol b) RON of FACE gasolines blended with ethanol c) MON of hydrocarbons blended with ethanol and d) MON of FACE gasolines blended with ethanol

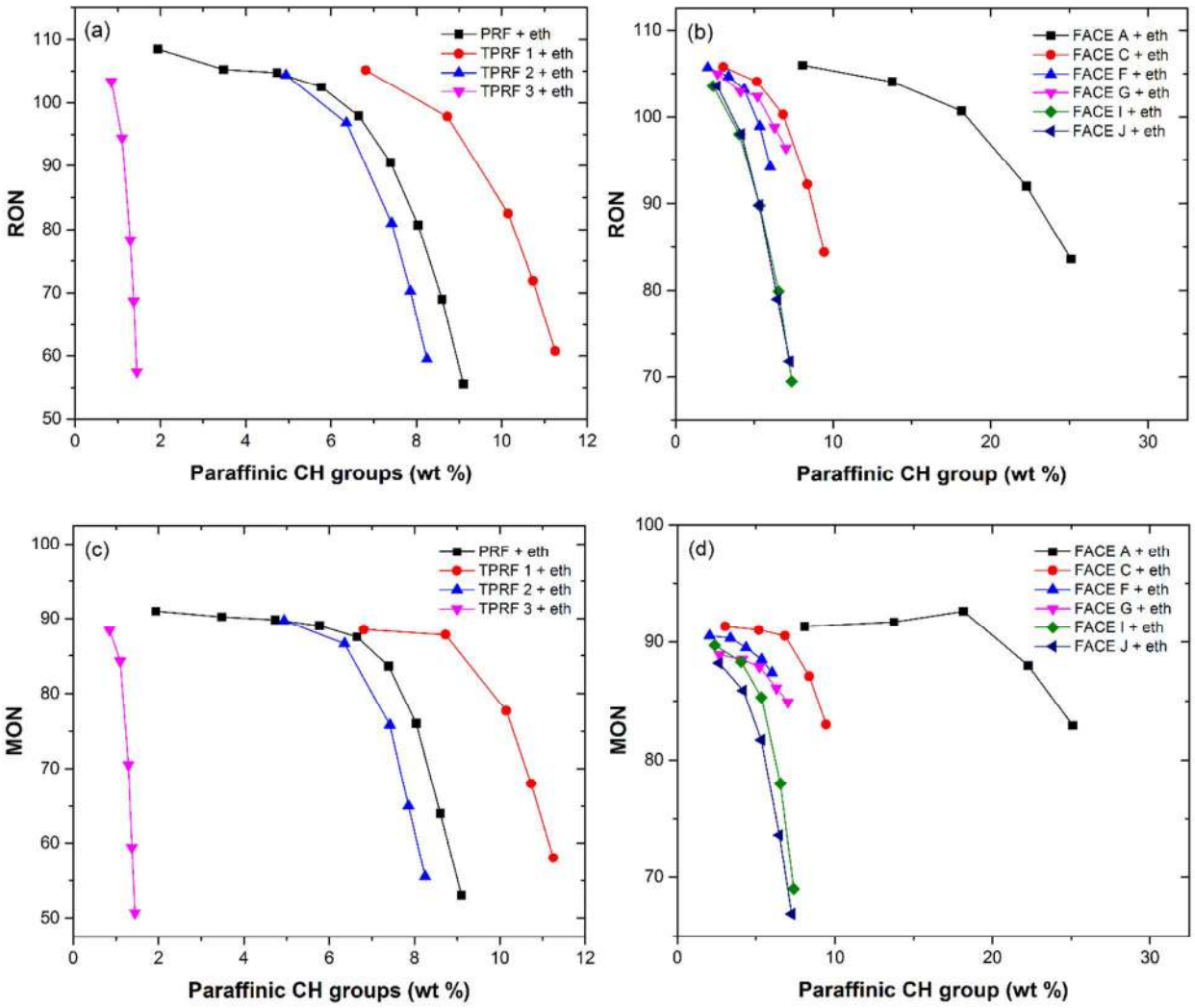

Figure 5. Effect of paraffinic CH groups on a) RON of hydrocarbons blended with ethanol b) RON of FACE gasolines blended with ethanol c) MON of hydrocarbons blended with ethanol and d) MON of FACE gasolines blended with ethanol

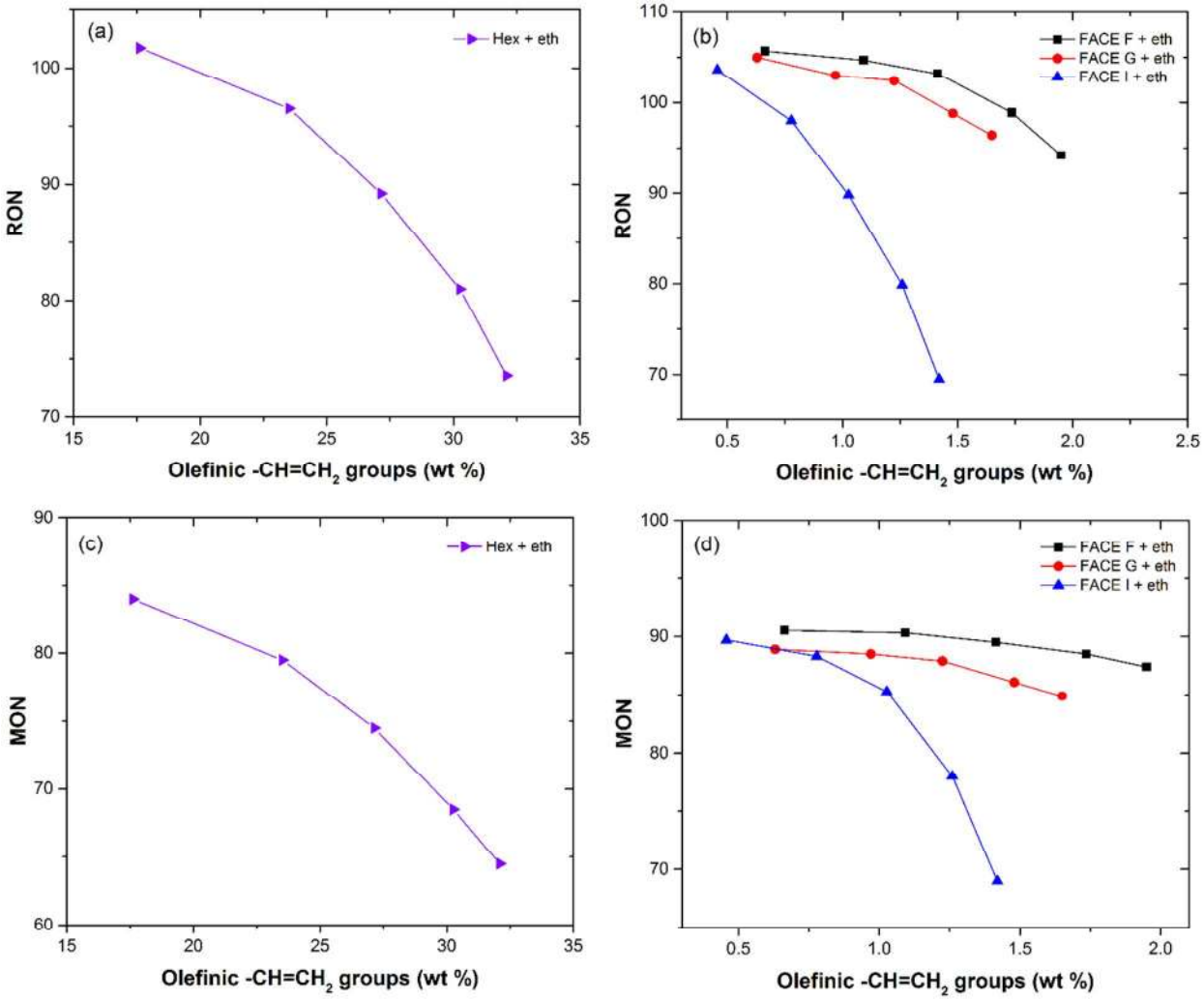

Figure 6. Effect of olefinic -CH=CH_2 groups on a) RON of hydrocarbons blended with ethanol b) RON of FACE gasolines blended with ethanol c) MON of hydrocarbons blended with ethanol and d) MON of FACE gasolines blended with ethanol

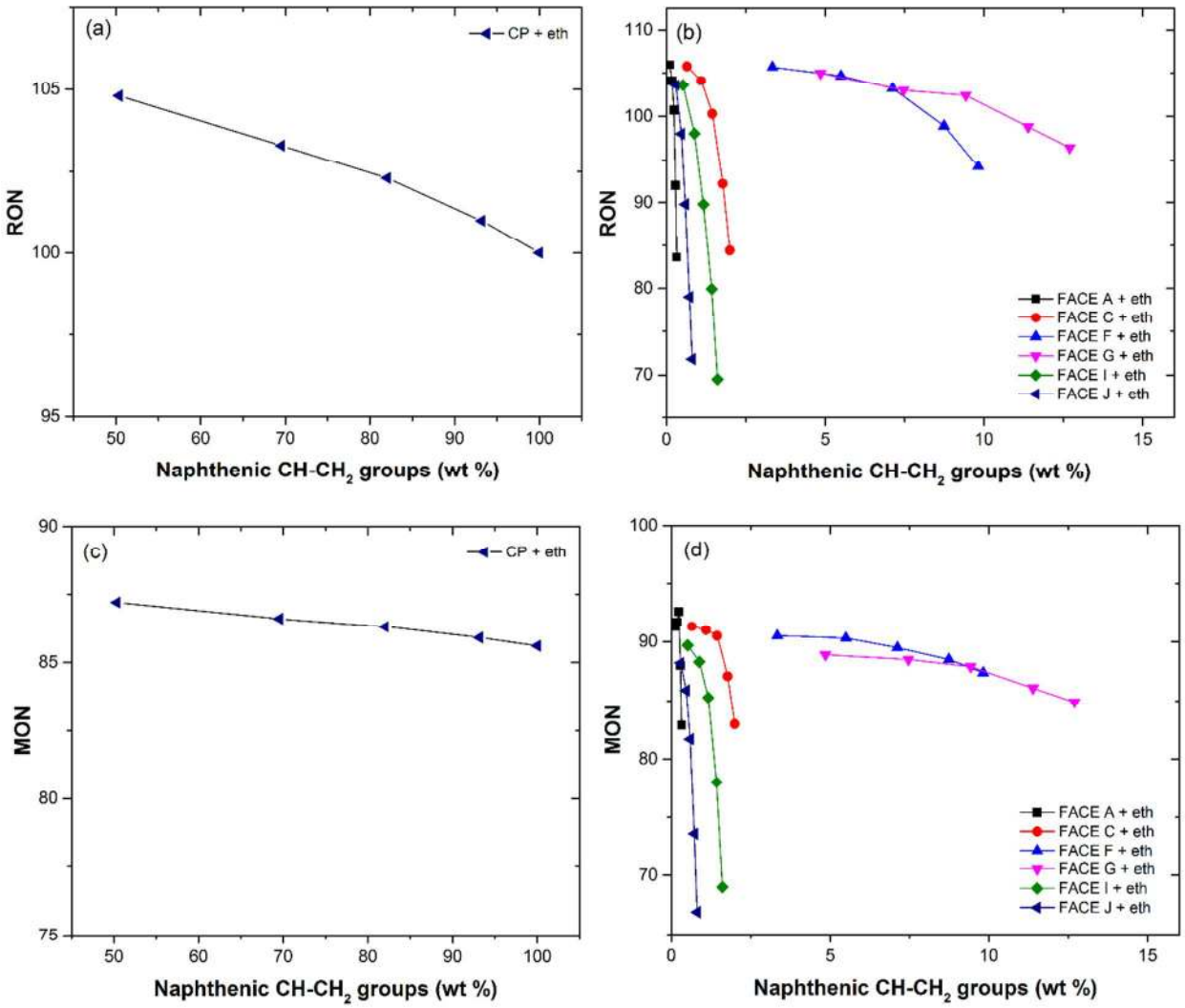

Figure 7. Effect of naphthenic CH-CH_2 groups on a) RON of hydrocarbons blended with ethanol b) RON of FACE gasolines blended with ethanol c) MON of hydrocarbons blended with ethanol and d) MON of FACE gasolines blended with ethanol

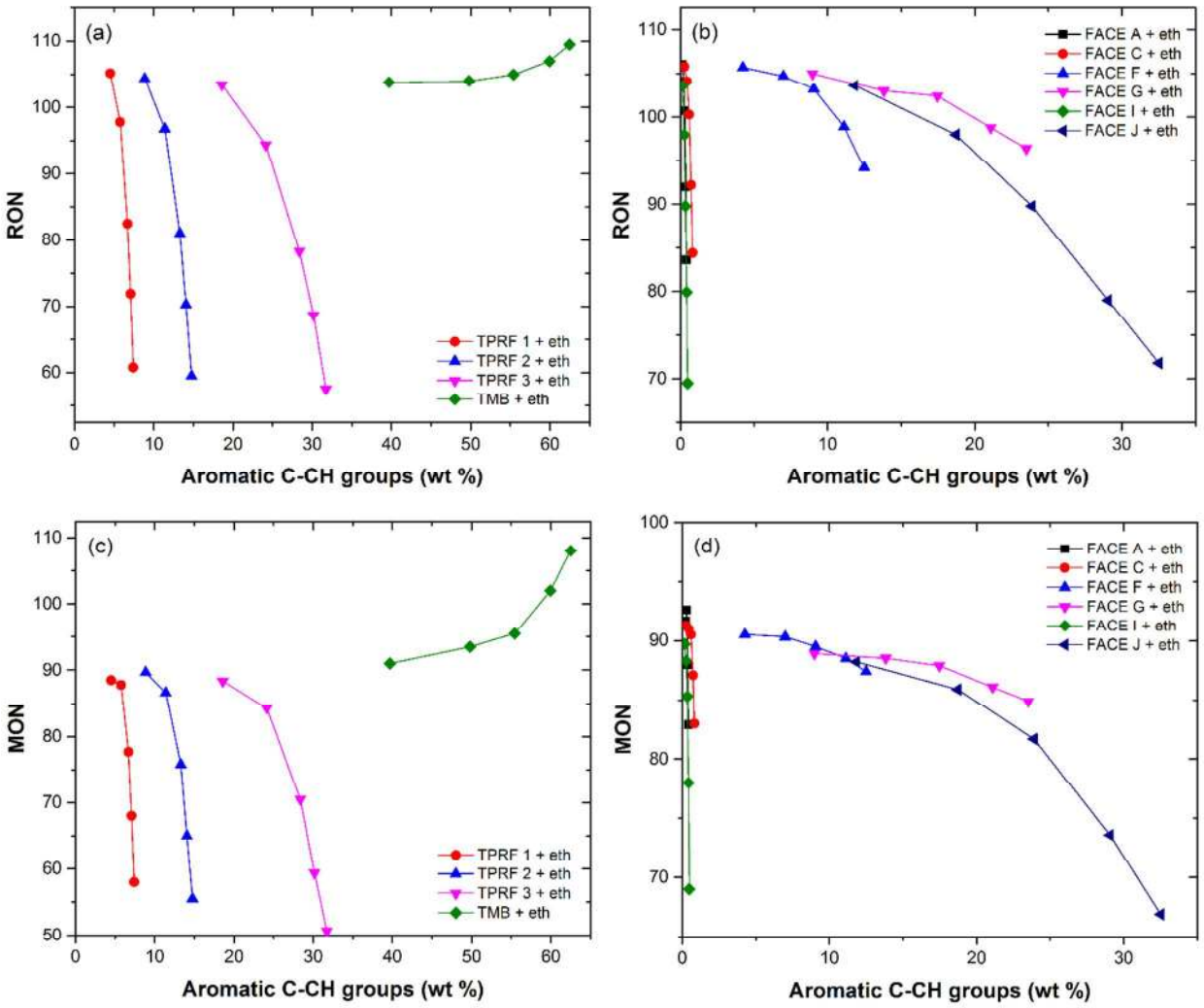

Figure 8. Effect of aromatic CH groups on a) RON of hydrocarbons blended with ethanol b) RON of FACE gasolines blended with ethanol c) MON of hydrocarbons blended with ethanol and d) MON of FACE gasolines blended with ethanol

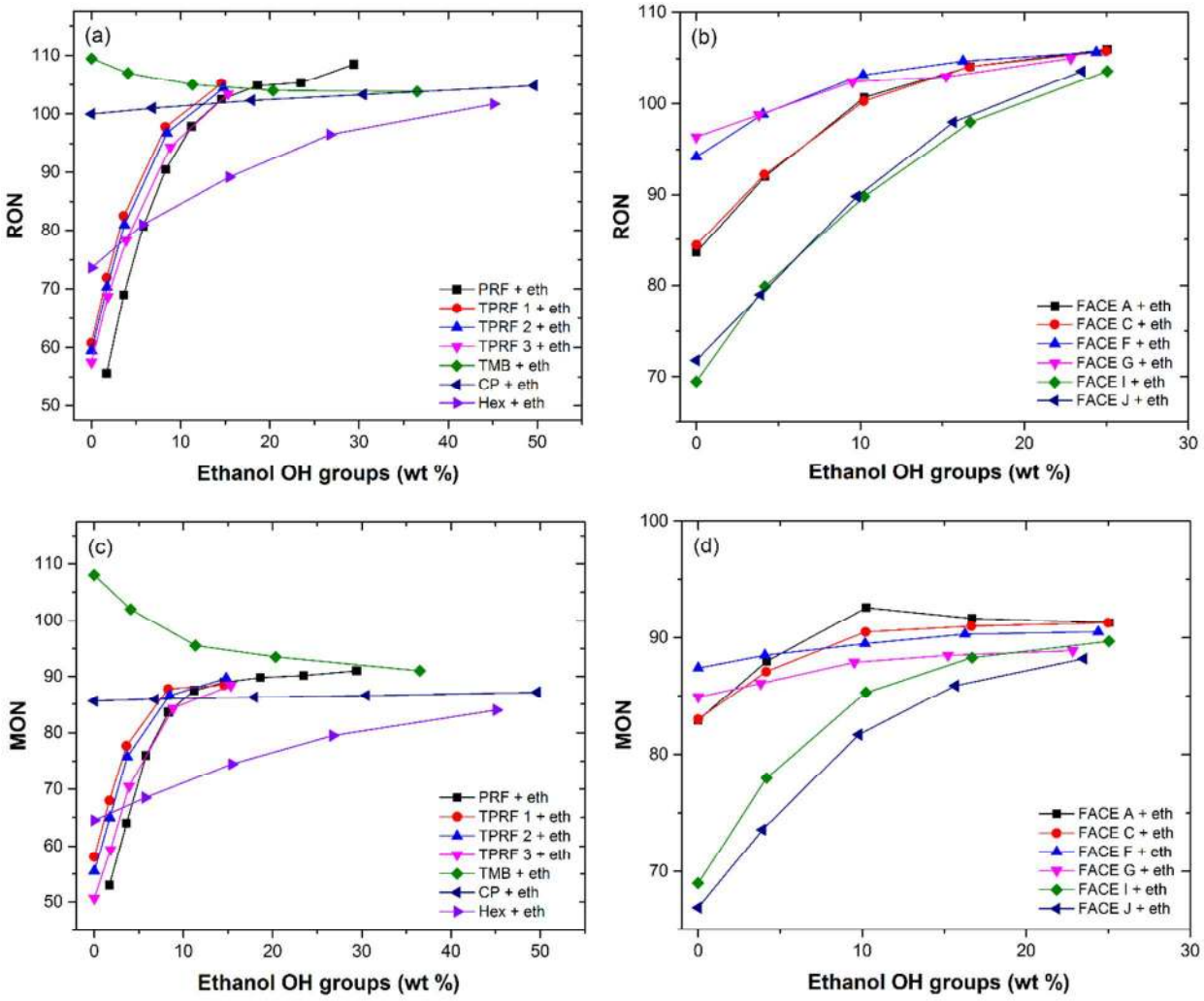

Figure 9. Effect of ethanol OH groups on a) RON of hydrocarbons blended with ethanol b) RON of FACE gasolines blended with ethanol c) MON of hydrocarbons blended with ethanol and d) MON of FACE gasolines blended with ethanol

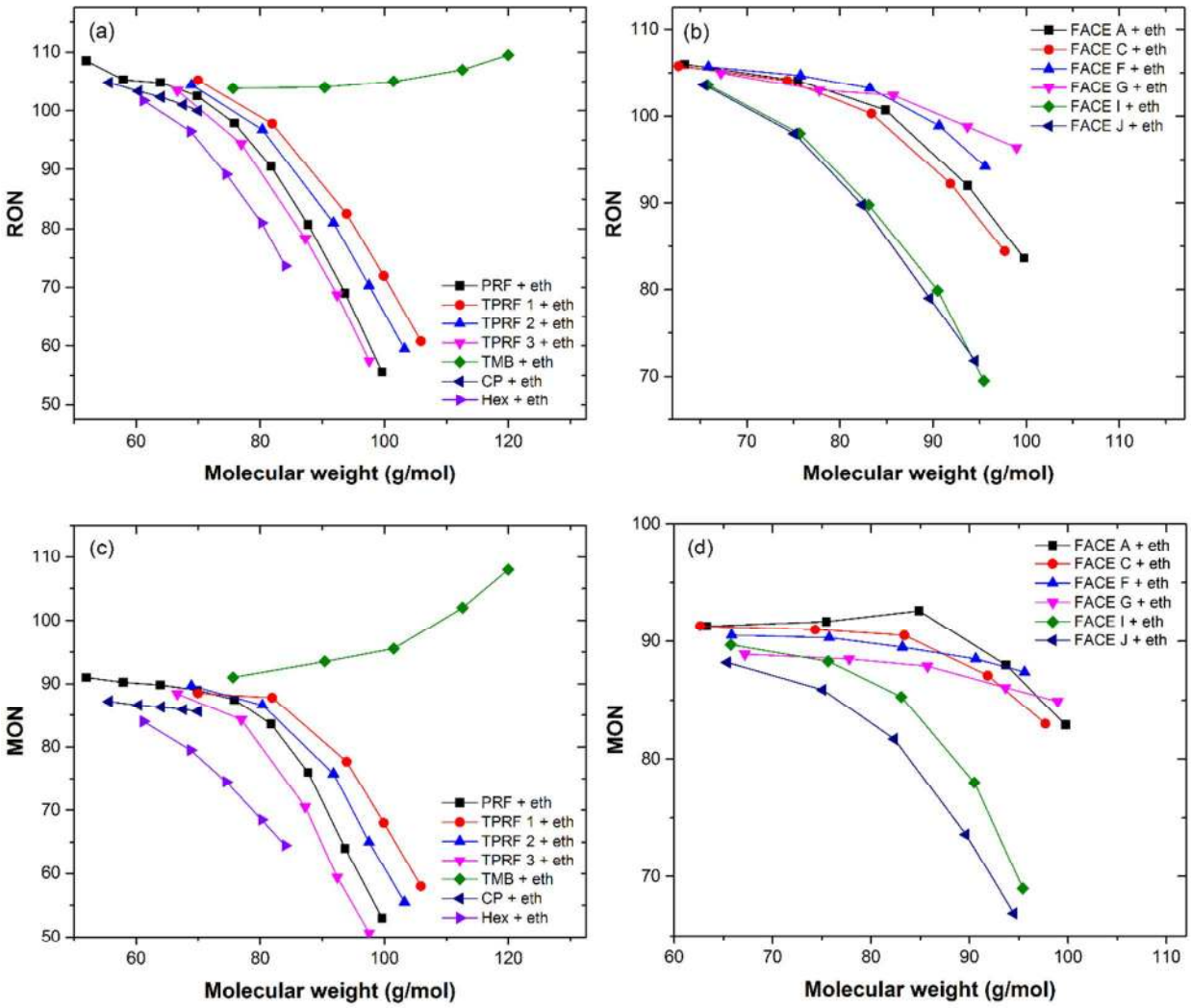

Figure 10. Effect of molecular weight on a) RON of hydrocarbons blended with ethanol b) RON of FACE gasolines blended with ethanol c) MON of hydrocarbons blended with ethanol and d) MON of FACE gasolines blended with ethanol

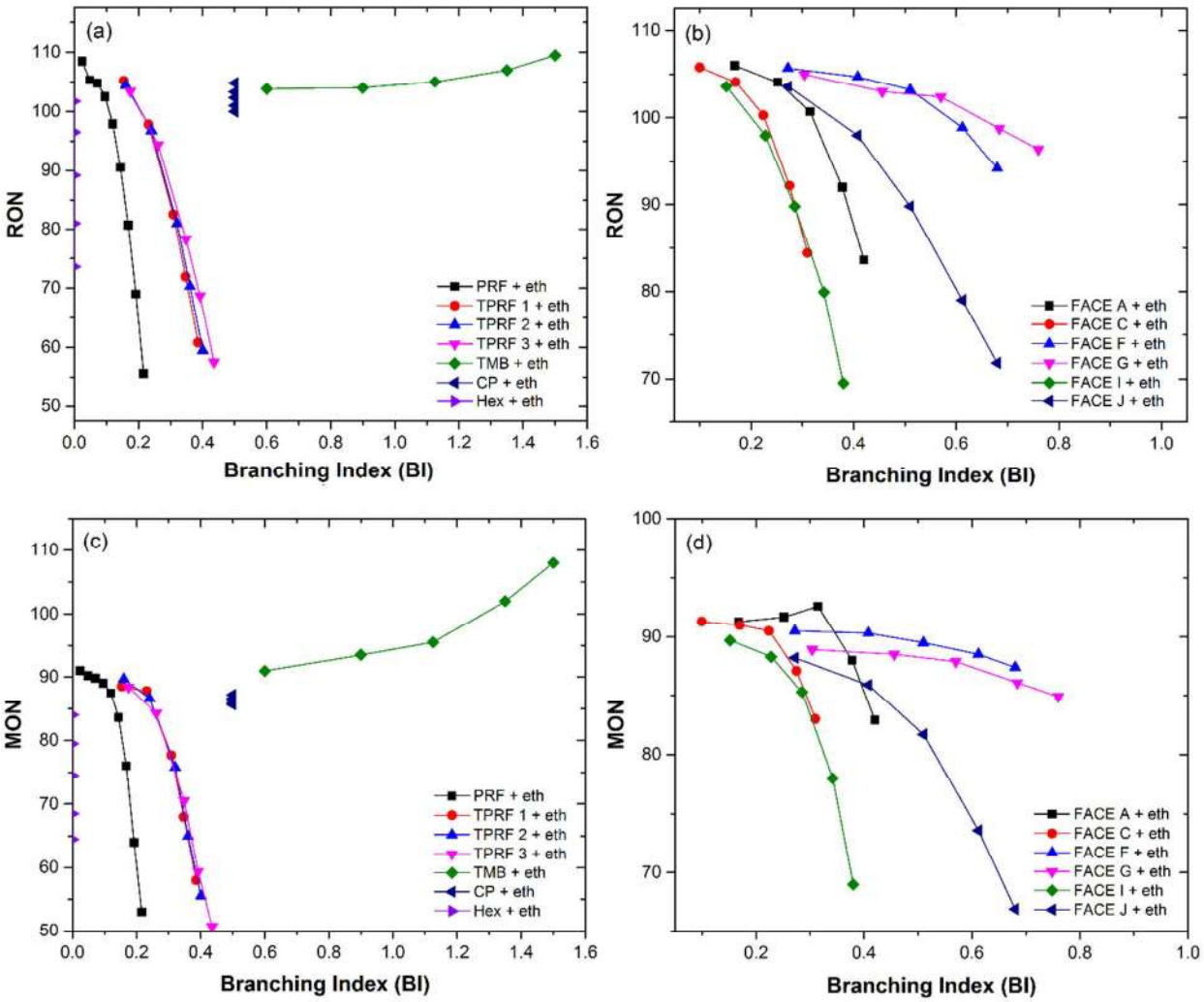

Figure 11. Effect of molecular weight on a) RON of hydrocarbons blended with ethanol b) RON of FACE gasolines blended with ethanol c) MON of hydrocarbons blended with ethanol and d) MON of FACE gasolines blended with ethanol

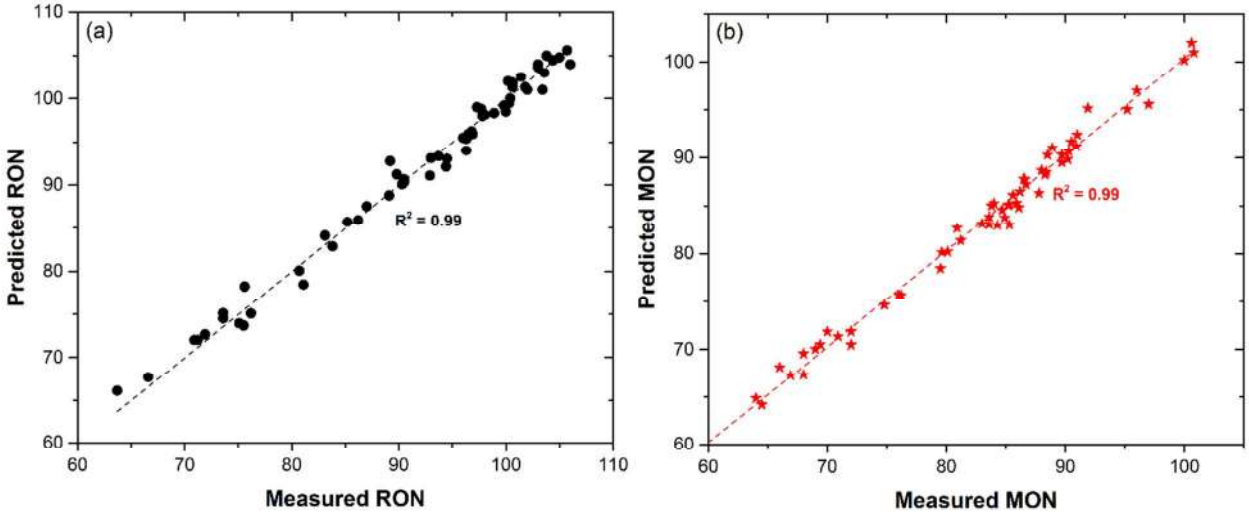

Figure 12. Comparison of measured and predicted RON and MON values using the ANN models

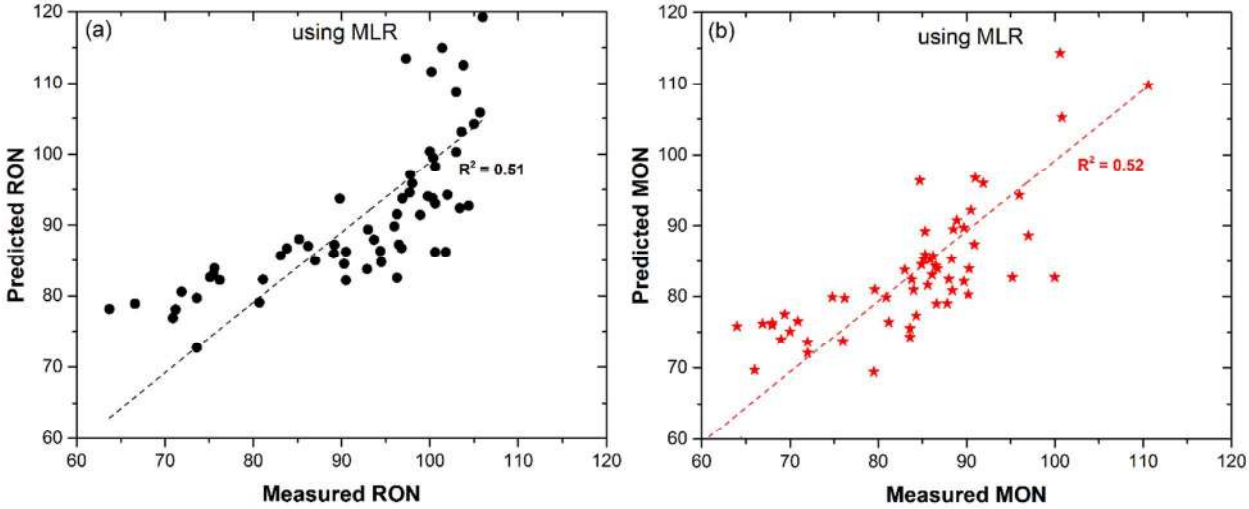

Figure 13. Comparison of measured and predicted RON and MON values using MLR

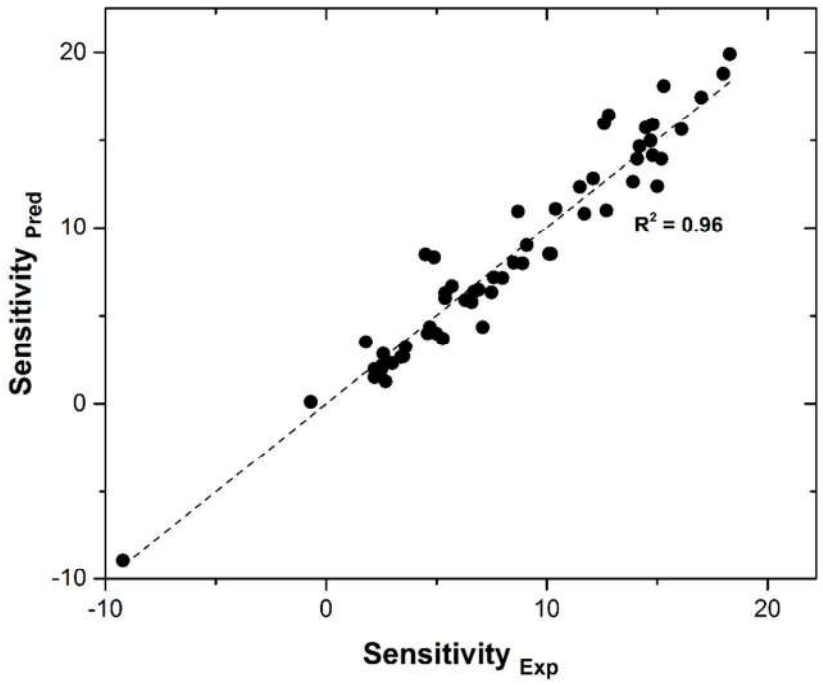

Figure 14. Comparison of measured and predicted sensitivity of the fuels